

Dear author,

Thank you for your detailed reply to the referees. Before accepting your manuscript for publication, I would like you to consider and answer the following remarks from my side (the page and line numbers correspond to the second word document you sent me off line).

We thank the editor for her careful monitoring and reading of our manuscript. We considered her final suggestions. A point-by-point reply is presented hereafter.

- Following the comment from Referee 2 on the large marine predator, you write that the forecasting system “will ultimately consist of 3 numerical models ...” as if it was not the case in the current study but you mention a separate paper to come. This seems contradictory to what is written in the manuscript “The model system consists of three models” as if it was the case in the current study - and you do not mention the paper to come. Please clarify.

Answer:

Yes, in the framework of INDESO project, the forecasting system consists of 3 numerical models. Ocean dynamics and biogeochemistry are part of the same NEMO system, and are running simultaneously (“online” mode). The fish population dynamics model is an external model as regard to NEMO. It uses the outputs of the two other models as external forcing’s.

- Following the comment from Referee 2 on the importance of “iron supply from river run off vs iron supply from sediments”, a sentence summarizing your “Author's response 4” should be added in the text.

Answer:

We added a sentence in Section 3.3 External inputs:

“A finer adaptation of each external source of nutrients is prevented by the crucial lack of in-situ measurements in the region of interest.”

- Author's response 7: from your reply, I understand that only MODIS is used; but from the text, I understand that both MODIS and MERIS are used. Please clarify.

Answer:

Sorry, I realize that my answer to Referee 2 was not very clear.

For the evaluation of the annual mean state (Section 5.1), we consider MODIS Case-1 and MERIS Case-2 products as they give different annual mean chlorophyll-a concentrations (year 2011) in the studied area.

For the evaluation of the seasonal cycle (Section 5.2) and interannual variability (Section 5.3), we are more interested in the amplitude and phasing between the model and satellite estimation. As well the end of MERIS sensor in April 2012 prevented us to use this sensor. It would have multiplied the figures and the explanations while it is not the objective of the section.

So, only MODIS is used for the complete evaluation of the model.

We added a sentence in Section 4.3 to clarify:
“... unfortunately the mission ended in April 2012. So MERIS is only used for the evaluation of the annual mean state.”

- On Figure 7, is r strictly equal to 0?

Answer:

Sorry, there was a problem with the rounding to the second decimal.
In Figure 7c, r is not strictly 0 but instead -0.01.
I checked and corrected this problem in the three Figures (7, 8, 9).

- p.8, L4: I do not understand what “respectively build using analytical values” means. Please clarify.

Answer:

Sorry, the sentence was not very clear.
We changed: “For tracers for which this information is missing, initial and open boundary conditions come either from a global scale simulation, are estimated from satellite data, respectively build using analytical values.” for “For tracers for which this information is missing, initial and open boundary conditions come either from a global scale simulation, are estimated from satellite data, or are build using analytical values.”

- p.1, L24: despite what you write in your reply, the word “degradation” is still used. This is fine with me but some explanations should be added on what “without degradation in space and time” means.

Answer:

Sorry. We removed the term “degradation” as it is not useful for the study, and we changed “NEMO-OPA physical ocean model and the PISCES biogeochemical model are coupled in “on-line” mode without degradation in space and time.” For “The NEMO-OPA physical ocean model and the PISCES biogeochemical model are running simultaneously (“on-line” coupling), at the same resolution.”

- p.8, 1st parag.: It would be better to move the sentence “Initial and open boundary conditions are summarized in Table 1.” at the beginning of the paragraph.

Answer:

We moved this sentence at the beginning of the paragraph.

- p.18, L21-22: To follow Referee 2's comment and your reply, I suggest to change “The strengths of the simulation are reminded below and weaknesses are discussed as follow: coastal ocean, cross-shore gradient and open ocean.” for “In the following paragraphs, the strengths of the simulation are first reviewed and weaknesses are then discussed.”

Answer:

We changed “The strengths of the simulation are reminded below and weaknesses are discussed as follow: coastal ocean, cross-shore gradient and open ocean.” for “In the following paragraphs, the strengths of the simulation are first reviewed and weaknesses are then discussed.”

Also for better readability, I suggest the following minor changes :

- p.3, L10: «leading to 80% of the reefs at risk» for «leading to 80% of the reefs being at risk»
- p.3, L27: “The regional configuration of ocean dynamics” for “The regional ocean dynamics”
- p.3, L30-31: “displays similar patterns to satellite estimates” for “displays patterns similar to satellite estimates”
- p.4, L9-10: please remove “(Section 5)” as it appears earlier in the sentence
- p.5, L17: “of waters which” for “of waters, which”
- p.6, L2-3: “effects of each climate mode are more difficult to analyse as both influence ITF transport” for “effects of ENSO and IOD climate modes are more difficult to discriminate as they both influence ITF transport”
- p.6, L17: “has especially been developed” for “has been developed especially”
- p.7, L17: “asselin filter” for “Asselin filter”
- p.7, L19 & 22: “ie.” for “i.e.”
- p.8, L4: “or they have to be estimated from satellite data” for “or are estimated from satellite data”
- Please use full name or symbols consistently. E.g. on p.8 L13-15, you use “iron” and not “Fe”, but later in the sentence you use the symbol “Si”
- p.8, L15: “Yearly river mean discharges” for “Yearly means of river discharges”
- p.9, L11: “we are using years 2010 to 2014” for “we use years 2010 to 2014”
- p.18, L16: “A suit of numerical models has been coupled “ for “A suite of numerical models were coupled” (a “suit” c'est un costume !)
- p.18, L18: “Here we access the skill” for “Here we assess the skill”
- p.18, L20: “was launched in January 2007” for “was launched starting in January 2007” (if not, it sounds as if the run really started 9 years ago)
- p.19, L4: “... Indian part). These anomalies suggest ...” for “... Indian part); this suggests ...” (because “anomalies” in its original sense sounds like something is wrong)
- p.19, L8: “deepened in a future study” for “further investigated”
- p.19, L9: “.Mean chlorophyll-a ...” for “However, mean chlorophyll-a ...” to mark the start of the section describing weaknesses.
- p.19, L.11: “are diffusive” for “are too diffusive”.
- p.19, L.15: “The slight disequilibrium introduced ...” for “The slight disequilibrium explicitly introduced ...”
- p.19, L.16: “in line with observations” for “and to make it comparable with observations.”
- p.19, L.20: “will be needed” for “is needed”
- p.19, L.20: “availability of data. Most of the” for “availability of data as most of the”
- p.19, L.20: please remove the comma in “too much chlorophyll-a, and NPP on the shelves”
- p. 20, L.11: “However, it results in an overestimation of the vertical gradient of nutrients, and the nutricline is considerably strengthened” for “However, it would result in an overestimation of the vertical gradient of nutrients, and the nutricline would be considerably strengthened”
- p. 20, L.13: “Improving ...” for “Hence improving ...”

- p. 20, L.15: “relies at first order on the model physics.” for “first requires improving the model physics.”
- p. 20, L.23: “initialized and forced by the same PSY3 forecasting system.” for “initialized and forced coherently, on the base of the PSY3 forecasting system.”

Answer:

We included all these changes in the text.

Remark:

To strictly match with Part 1:

“Evaluation of an operational ocean model configuration at 1/12° spatial resolution for the Indonesian seas (NEMO2.3/INDO12) – Part 1: Ocean physics”

We changed the title to:

“Evaluation of an operational ocean model configuration at 1/12° spatial resolution for the Indonesian seas (NEMO2.3/INDO12) - Part 2: Biogeochemistry”

Evaluation of an operational ocean model configuration at 1/12° spatial resolution for the Indonesian seas (NEMO2.3/INDO12) ~~Part #1~~ Part #2: Biogeochemistry

E. Gutknecht¹, G. Reffray¹, M. Gehlen², I. Triyulianti³, D. Berlianty³, and P. Gaspar⁴

[1]{Mercator Ocean, 8-10 rue Hermès, 31520 Ramonville, France}

[2]{LSCE, UMR CEA-CNRS-UVSQ, Saclay, L'Orme des Merisiers, 91191 Gif-sur-Yvette, France}

[3]{Institute for Marine Research and Observation, Jl. Baru Perancak, Negara-Jembrana, Bali 82251, Republic of Indonesia}

[4]{CLS, 8-10 rue Hermès, 31520 Ramonville, France}

Correspondence to: E. Gutknecht (elodie.gutknecht@mercator-ocean.fr)

Abstract

In the framework of the INDES0 (Infrastructure Development of Space Oceanography) project, an operational ocean forecasting system was developed to monitor the state of the Indonesian seas in terms of circulation, biogeochemistry and fisheries. This forecasting system combines a suite of numerical models connecting physical and biogeochemical variables to population dynamics of large marine predators (tunas). The physical/biogeochemical coupled component (the INDO12BIO configuration) covers a large region extending from the Western Pacific Ocean to the Eastern Indian Ocean at 1/12° horizontal resolution. The ~~OPA/NEMO-OPA~~ physical ocean model and the PISCES biogeochemical model are running simultaneously (“on-line” coupling), at the same resolution. coupled in “on-line” mode without degradation in space and time. The operational global ocean forecasting system (1/4°) operated by Mercator Ocean provides the physical forcing, while climatological open boundary conditions are prescribed for the biogeochemistry.

This paper describes the skill assessment of the INDO12BIO configuration. Model skill is assessed by evaluating a reference hindcast simulation covering the last 8 years (2007-2014). Model results are compared to satellite, climatological and *in-situ* observations. Diagnostics are performed on nutrients, oxygen, chlorophyll-*a*, net primary production, and mesozooplankton.

The model reproduces large scale distributions of nutrients, oxygen, chlorophyll-*a*, NPP-net primary production and mesozooplankton biomasses. Modelled vertical distributions of nutrients and oxygen are comparable to *in-situ* datasets although gradients are slightly smoothed. The model simulates realistic biogeochemical characteristics of North Pacific tropical waters entering in the archipelago. Hydrodynamics transformation of water masses across the Indonesian archipelago allows conserving nitrate and oxygen vertical distribution close to observations, in the Banda Sea and at the exit of the archipelago. While the model overestimates the mean surface chlorophyll-*a*, the seasonal cycle is in phase with satellite estimations, with higher chlorophyll-*a* concentrations in the southern part of the archipelago during SE monsoon, and in the northern part during NW monsoon. The time-series of chlorophyll-*a* anomalies suggests that meteorological and ocean physical processes that drive the interannual variability of biogeochemical properties in the Indonesian region are reproduced by the model.

1 Introduction

The “Coral triangle” delineated by Malaysia, the Philippines, New Guinea, Solomon Islands, East-Timor and Indonesia is recognized as a global hotspot of marine biodiversity (Allen and Werner, 2002; Mora et al., 2003; Green and Mous, 2004; Allen, 2008). It gathers 20% of the world’s species of plants and animals, and the greatest concentration and diversity of reefs (76% of the world’s coral species; Veron et al., 2009). The Indonesian archipelago is located at the centre of this ecologically rich region. It is characterized by a large diversity of coastal habitats such as mangrove forests, coral reefs and sea grass beds, all of which shelter ecosystems of exceptional diversity (Allen and Werner, 2002). The archipelago's natural heritage represents an important source of income and employment, with its future critically depending on the sustainable management of ecosystems and resources (e.g. Foale et al., 2013; Cros et al., 2014).

The wider Coral Triangle and its sub-region, the Indonesian archipelago, are facing multiple threats resulting from demographic growth, economic development, change in land use practices and deforestation, as well as global climate change (<http://www.metoffice.gov.uk/media/pdf/8/f/Indonesia.pdf>; FAO, 2007). Human activities cause changes in the delivery of sediments, nutrients and pollutants to coastal waters, leading to eutrophication, ecosystem degradation, as well as species extinctions (Ginsburg, 1994; Pimentel et al., 1995; Bryant et al., 1998; Roberts et al., 2002; UNEP, 2005; Alongi et al., 2013). Surveys report an over 30% reduction of mangroves in Northern Java over the last 150 years and an increase of coral reef degradation from 10% to 50% in the last 50 years (Bryant et al., 1998; Hopley and Suharsono, 2000; UNEP, 2009), leading to 80% of the reefs **being** at risk in this region (Bryant et al., 1998). These changes not only damage coastal habitats, but also propagate across the whole marine ecosystem from nutrients and the first levels of the food web up to higher trophic levels, along with concomitant changes in biogeochemical cycles.

There is thus a vital need for monitoring and forecasting marine ecosystem dynamics. The INDESO project (Infrastructure Development of Space Oceanography, www.indeso.web.id/indeso_wp/index.php), funded by the Indonesian Ministry of Marine Affairs and Fisheries, aims at the development of sustainable fishery practices in Indonesia, the monitoring of its Exclusive Economic Zone (EEZ) and the sustainable management of its ecosystems. The project addresses the Indonesian need for building a national capability for operational oceanography. The model system consists of three models deployed at the scale of the Indonesian archipelago: an ocean circulation model (NEMO-OPA; Madec, 2008), a biogeochemical model (PISCES; Aumont and Bopp, 2006) with a spatial resolution of 1/12°, as well as an intermediate trophic level/fish population dynamics model (SEAPODYM; Lehodey et al., 2008). Since mid-September 2014, the chain of models is fully operational in Perancak (Bali, Indonesia) and delivers 10-day forecast / two weeks hindcast on a weekly basis (see <http://www.indeso.web.id>).

The regional ~~configuration of~~ ocean dynamics is fully described in Tranchant et al. (this volume, hereafter Part 1). The physical model reproduces main processes occurring in this complex oceanic region. Ocean circulation and water mass transformation through the Indonesian Archipelago are close to observations. Eddy Kinetic Energy displays **patterns**

similar ~~patterns~~ to satellite estimates, tides being a dominant forcing in the area. The volume transport of the Indonesian ThroughFlow is comparable to INSTANT data. TS diagrams highlight the erosion of South and North Pacific subtropical waters while crossing the archipelago.

The present paper (Part 2) focuses on ocean biogeochemistry. It is organized as follows. The next section presents an overview of the area of study with emphasis on main drivers of biological production over the Indonesian archipelago. The biogeochemical component of the physical-biogeochemical coupled configuration is described in Section 3. Satellite, climatological and *in-situ* observations used to evaluate simulation results are detailed in Section 4. Section 5 presents the evaluation of the skill of the coupled model to reproduce main biogeochemical features of Indonesian seas along with their seasonal and interannual dynamics (~~Section 5~~). Finally, discussion and conclusion are presented in Section 6.

2 Area of study

The Indonesian archipelago is crossed by North and South Pacific waters that converge in the Banda Sea, and leave the archipelago through three main straits: Lombok, Ombai and Timor. This ocean current (Indonesian ThroughFlow; ITF) provides the only low-latitude pathway for warm, fresh waters to move from the Pacific to the Indian Ocean (Gordon, 2005; Hirst and Godfrey, 1993). On their way through the Indonesian archipelago, water masses are progressively transformed by surface heat and freshwater fluxes and intense vertical mixing linked to strong internal tides trapped in the semi-enclosed seas as well as upwelling processes (Field and Gordon, 1992). The main flow, as well as the transformation of Pacific waters is correctly reproduced by the physical model, with a realistic distribution of the volume transport through the three major outflow passages (Part 1). In the Indian Ocean, this thermocline water mass forms a cold and fresh tongue between 10°S and 20°S, and supplies the Indian Ocean with nutrients. These nutrients impact biogeochemical cycles and support new primary production in the Indian Ocean (Ayers et al., 2014).

Over the archipelago, complex meteorological and oceanographic conditions drive the distribution and growth of phytoplankton and provide favourable conditions for the development of a diverse and productive food web extending from zooplankton, and

intermediate trophic levels to pelagic fish (Hendiarti et al., 2004, 2005; Romero et al., 2009). The tropical climate is characterized by a monsoon regime and displays a well-marked seasonality. The south-east (SE) monsoon (April to October) is associated with easterlies from Australia that carry warm and dry air over the region. Wind-induced upwelling along the southern coasts of Sumatra, Java and Nusa-Tenggara Islands (hereafter named Sunda Islands) and in the Banda Sea is associated with high chlorophyll-*a* levels (Susanto et al., 2006; Rixen et al., 2006). Chlorophyll-*a* maxima along Sunda Islands move to the west over the period of the SE monsoon, in response to the alongshore wind shift and associated movement of the upwelling centre (Susanto et al., 2006). From October to April, the north-west (NW) monsoon is associated with warm and moist winds from the Asian continent. Winds blow in a south-west direction north of the Equator and towards Australia south of the Equator. They generate a downwelling and a reduced chlorophyll-*a* content south of the Sunda Islands and in the Banda Sea. The NW monsoon also causes some of the highest precipitation rates in the world. Increased river runoff carries important sediment loads (20 to 25% of the global riverine sediment discharge; Milliman et al., 1999), along with carbon and nutrients to the ocean. These inputs are a strong driver of chlorophyll-*a* variability and play a key role in modulating the biological carbon pump across Indonesian seas (Hendiarti et al., 2004; Rixen et al., 2006). High levels of suspended matter decrease the water transparency in coastal areas and modify the optical properties of waters, which in turn interferes with ocean colour remote sensing (Susanto et al., 2006). Although several Indonesian rivers are classified among the 100 most important rivers of the world, most of them are not regularly monitored. It is thus currently impossible to estimate the impact of river runoff on the variability of chlorophyll-*a* in the region (Susanto et al., 2006).

Indonesian seas are also greatly influenced by modes of natural climate variability owing to its position on the equator between Asia and Australia and between the Pacific and Indian Oceans. Strength and timing of the seasonal monsoon are modulated by interannual phenomena that disturb atmospheric conditions and ocean currents. A significant correlation between the variability of the Indonesian ThroughFlow (ITF) and the El Niño-Southern Oscillation (ENSO) was reported (e.g. Meyers, 1996; Murtugudde et al., 1998; Potemra et al., 1997), with ENSO modulating rainfall and chlorophyll-*a* on inter-annual timescales (Susanto et al., 2001, 2006; Susanto and Marra, 2005). [ENSO can be monitored using a Multivariate](#)

[ENSO Index \(MEI; Wolter and Timlin, 1993, 1998; http://www.esrl.noaa.gov/psd/enso/mei/\)](http://www.esrl.noaa.gov/psd/enso/mei/).

In the Eastern Indian Ocean, large anomalies off Sumatra and Java coasts are associated with the Indian Ocean Dipole (IOD) Mode monitored via the Dipole Mode Index (DMI; Saji et al., 1999). A strong positive index points to abnormally strong coastal upwelling and a large phytoplankton bloom near Java Island (Meyers, 1996; Murtugudde et al., 1999). Inside the archipelago, ~~effects of each climate mode are more difficult to analyse as both influence ITF transport.~~ effects of ENSO and IOD climate modes are more difficult to discriminate as they both influence ITF transport. There is, however, evidence for Indian Ocean dynamics to dominate over Pacific Ocean dynamics as drivers of ITF transport variability (Masumoto, 2002; Sprintall and Révelard, 2014).

Finally, tides, the Madden-Julian Oscillation, Kelvin and Rossby waves are additional drivers of variability across Indonesian seas and influence marine ecosystems (Madden and Julian, 1994; Field and Gordon, 1996; Sprintall et al., 2000; Susanto et al., 2000, 2006).

3 The INDO12BIO configuration

3.1 The coupled model

In the framework of the INDESIO project, a physical-biogeochemical coupled model is deployed over the domain from 90°E-144°E to 20°S-25°N, widely encompassing the whole Indonesian archipelago, with a spatial resolution of 1/12°. The physical model is based on the NEMO-OPA 2.3 circulation model (Madec et al., 1998; Madec, 2008). Specific improvements include time-splitting and non-linear free surface to correctly simulate high frequency processes such as tides. A parameterization of the vertical mixing induced by internal tides has ~~especially~~ been developed especially for NEMO-OPA (Koch-Larrouy et al., 2007, 2010) and is used here. The physical configuration called INDO12 is described in detail in Part I1 ~~(Tranchant et al., this volume)~~.

Dynamics of biogeochemical properties across the area are simulated by the PISCES model version 3.2 (Aumont and Bopp, 2006). PISCES simulates the first levels of the marine food web from nutrients up to mesozooplankton. It has 24 state variables. PISCES considers five limiting nutrients for phytoplankton growth (nitrate and ammonium, phosphate, dissolved

Ssilica and iron). Four living size-classified compartments are represented: two phytoplankton groups (nanophytoplankton and diatoms) prognostically predicted in cCarbon (C), ironFe (Fe), Ssilica (Si) (the latter only for diatoms) and chlorophyll content, and two zooplankton groups (microzooplankton and mesozooplankton). Constant C/N/P Redfield ratios are supposed for all species. While internal Fe/C and Si/C ratios of phytoplankton are modelled as a function of the external availability of nutrients and thus variable, only C is prognostically modelled for zooplankton. The model includes five non-living compartments: small and big particulate organic carbon and semi-labile Ddissolved eOrganic Ccarbon (DOC), particulate inorganic carbon (CaCO₃ as calcite) and biogenic silica. PISCES also simulates Dissolved Inorganic Carbon (DIC), total alkalinity (carbonate alkalinity + borate + water), and dissolved oxygen. The CO₂ chemistry is computed following the OCMIP protocols (<http://ocmip5.ipsl.jussieu.fr/OCMIP/>). Biogeochemical parameters are based on the standard PISCES namelist version 3.2. Please refer to Aumont and Bopp (2006) for a comprehensive description of the model (version 3.2).

PISCES is coupled to NEMO-OPA via the TOP component that manages the advection/diffusion equations of passive tracers and biogeochemical source and sink terms. In our regional configuration, called INDO12BIO, physics and biogeochemistry are running simultaneously (“on-line” coupling), at the same resolution. Particular attention must be paid to respect a number of fundamental numerical constraints. 1/ The numerical scheme of PISCES for biogeochemical processes is forward in time (Euler), which does not correspond to the classical leap-frog scheme used for the physical component. Moreover, the free surface explicitly solved by the time splitting method is non linear. In order to respect the conservation of the tracers, the coupling between biogeochemical and physical components is done every second time step. As a result, the biogeochemical model is controlled by only one leap-frog trajectory of the dynamical model. The use of an aAsselin filter allows keeping the two numerical trajectories close enough to overcome this shortcoming. The advantage is a reduction of numerical cost and a time step for the biogeochemical model twice that of the physical component i.e. 900 seconds. 2/ As this time step is small, no time-splitting was used in the sedimentation scheme. 3/ The advection scheme is the standard scheme of TOP-PISCES i.e. the Monotonic Upstream centered Scheme for Conservation Laws (MUSCL)

(Van Leer, 1977). No explicit diffusion has been added as the numerical diffusion introduced by this advection scheme is already important.

3.2 Initial and open boundary conditions

The simulation starts on January 3rd, 2007 from the global ocean forecasting system at 1/4° operated by Mercator Ocean (PSY3 described in Lellouche et al., 2013) for temperature, salinity, currents, and free surface at the same date. Open boundary conditions (OBC) are also provided by daily outputs of this system. A 1° thick buffer layer allows nudging the signal at the open boundaries.

~~For biogeochemistry, initial and open boundary conditions are summarized in Table 1. Initial and open boundary conditions are derived from climatological data sets for nNitrate, phosphate, dissolved Si-silica, oxygen, dissolved inorganic carbon DIC, and alkalinity are derived from climatological data sets.~~ For tracers for which this information is missing, initial and open boundary conditions come either from a global scale simulation, ~~or they have to be~~ are estimated from satellite data, ~~respectively or are~~ build using analytical values. The global scale model NEMO-OPA/PISCES has been integrated for 3000 years at 2° horizontal resolution, until PISCES reached a quasi steady-state (see Aumont and Bopp, 2006). A monthly climatology was built for dissolved iron and DOC based on this simulation. ~~Initial and open boundary conditions are summarized in Table 1.~~ A Dirichlet boundary condition is used to improve the information exchange between the OBC and the interior of the domain.

3.3 External inputs

Three different sources are supplying the ocean in nutrients: atmospheric dust deposition, sediment mobilization, and rivers. Atmospheric deposition of iron comes from the climatological monthly dust deposition simulated by the model of Tegen and Fung (1995), and that of Si-silica follows Moore et al. (2002). Yearly means of river mean-discharges are taken from the Global Erosion Model (GEM) of Ludwig et al. (1996) for DIC, and from the Global News 2 climatology (Mayorga et al., 2010) for nutrients. An iron source corresponding to sediment reductive mobilization on continental margins is also considered. For more details on external supply of nutrients, please refer to the supplementary material of

Aumont and Bopp (2006). A finer adaptation of each external source of nutrients is prevented by the crucial lack of *in-situ* measurements in the region of interest.

In PISCES, external input fluxes are compensated by a loss to the sediments as particulate organic matter, biogenic ~~Si~~-silica and CaCO_3 . These fluxes correspond to matter definitely lost from the ocean system. The compensation of external input fluxes through output at the lower boundary closes the mass balance of the model. While such ~~an~~-equilibrium is a valid assumption at the scale of the global ocean, it is not reached at regional scale. For the INDO12BIO configuration, a decrease of the nutrient and carbon loss to the sediment was introduced corresponding to an increase in the water column remineralization by ~4%. This slight enhancement of water column remineralization leads to higher coastal chlorophyll-*a* concentrations (about +1 mg Chl m^{-3}) and enables the model to reproduce the chlorophyll-*a* maxima observed along the coasts of Australia and East Sumatra (not shown).

3.4 Simulation length

The simulation starts ~~see~~ on January 3rd, 2007 and operates up to present day as the model currently delivers ocean forecasts. For the present paper, we will analyse the simulation up to December 31, 2014. The spin-up length depends on the biogeochemical tracer (Fig. 1). The total carbon inventory computed over the domain (defined as the sum of all solid and dissolved organic and inorganic carbon fractions, yet dominated by the contribution of DIC) equilibrates within several months. To the contrary, ~~Dissolved Organic Carbon~~ (DOC), phosphate (PO_4) and ~~i~~Iron (Fe) need several years to stabilize (Fig. 1). The annual mean for year 2011 is used for comparison to satellite products (chlorophyll-*a*, net primary production). For comparison to climatologies (zooplankton, nutrients, oxygen) and analysis of the seasonal cycle, we ~~are using~~ years 2010 to 2014. Interannual variability is assessed over the whole length of simulation except the first year (2008 to 2014).

4 Satellite, climatological and *in-situ* data

Model outputs are compared to satellite, climatological, and *in-situ* observations. These observational data are detailed and described in this section.

4.1 INDOMIX cruise

The INDOMIX cruise on-board Marion Dufresne RV (Koch-Larrouy et al., in revision) crossed the Indonesian archipelago between the 09th and 19th of July 2010, and focused on one of the most energetic sections for internal tides from Halmahera Sea to Ombai Strait. Repeated CTD profiles over 24 hours as well as measurements of oxygen and nutrients were obtained for six stations at the entrance of the archipelago (Halmahera Sea), in the Banda Sea and in the Ombai Strait (three of them are used for validation; cf stations on Fig. 4). This data set provides an independent assessment of model skill. To co-localise model and observations, we took the closest simulated point to the coordinates of the station. 2-day model averages were considered as measurements were performed during 2 consecutive days at the stations selected for validation.

4.2 Nutrients and Oxygen

Modelled nutrient and oxygen distributions are compared to climatological fields of World Ocean Atlas 2009 (WOA 2009, 1° spatial resolution) (Garcia et al., 2010a, 2010b), respectively, the CSIRO Atlas of Regional Seas 2009 (CARS 2009, 0.5° spatial resolution) and discreet observations provided by the World Ocean Database 2009 (WOD 2009). Only nitrate, dissolved ~~Si~~-silica and oxygen distributions are presented hereafter. Nitrate + ammonium and phosphate are linked by a Redfield ratio in PISCES.

4.3 Chlorophyll-*a*

The ocean colour signal reflects a combination of chlorophyll-*a* content, suspended matter, coloured dissolved organic matter (CDOM) and bottom reflectance. Singling out the contribution of phytoplankton's chlorophyll-*a* is not straightforward in waters for which the relative optical contribution of the three last components is significant. This is the case over vast areas of the Indonesian archipelago where river discharges and shallow water depths contribute to optical properties (Susanto et al., 2006). The interference with optically absorbing constituents other than chlorophyll-*a* results in large uncertainties in coastal waters (up to 100%, as compared to 30% for open ocean waters) (Moore et al., 2009). Standard algorithms distinguish between open ocean waters / clear waters (Case-1) and coastal waters / turbid waters (Case-2). The area of deployment of the model comprises waters of both

categories and the comparison between modelled chlorophyll-*a* and estimates derived from remote sensing can be only qualitative. Two single-mission monthly satellite products are used for model skill evaluation. MODIS-Aqua (EOS mission, NASA) Level-3 Standard Mapped Image product (NASA Reprocessing 2013.1) covers the whole simulated period (2007-2014). It is a product for Case-1 waters, with a 9 km resolution, and is distributed by the ocean colour project (<http://oceancolor.gsfc.nasa.gov/cms/>). The MERIS (ENVISAT, ESA) L3 product (ESA 3rd reprocessing 2011) is also considered. Its spectral characteristics allow the use of an algorithm for Case-2 waters (MERIS C2R Neural Network algorithm; Doerffer and Schiller, 2007). It has a 4 km resolution and is distributed by ACRI-ST (<http://www.acri-st.fr/>), unfortunately the mission ended in April 2012. So MERIS is only used for the evaluation of the annual mean state.

4.4 Net primary production

Net primary production (NPP) is at the base of the food-chain. *In-situ* measurements of ~~primary production~~ NPP are sparse and we rely on products derived from remote sensing for model evaluation. The link between pigment concentration (chlorophyll-*a*) and carbon assimilation reflects the distribution of chlorophyll-*a* concentrations, but also the uncertainty associated to the production algorithm and the ocean colour product. At present, the community uses three production models. The Vertically Generalized Production Model (VGPM) (Behrenfeld and Falkowski, 1997) estimates vertically integrated NPP as a function of chlorophyll, available light, and photosynthetic efficiency. It is currently considered as the Standard algorithm. The two alternative algorithms are an "Eppley" version of the VGPM (distinct temperature-dependent description of photosynthetic efficiencies) and the Carbon-based Production Model (CbPM; Behrenfeld et al. 2005, Westberry et al. 2008). The latter estimates phytoplankton carbon concentration from remote sensing of particulate scattering coefficients. A complete description of the products is available at www.science.oregonstate.edu/ocean.productivity. Henson et al. (2010) point to the uncertainty of the CbPM algorithm, which yields results that are substantially different from the other algorithms. However On other hand, Emerson (2014) recommends the CbPM algorithm for providing the best results when tested at three time series sites (BATS, HOTS and OSP stations). ~~A complete description of the products is available at www.science.oregonstate.edu/ocean.productivity.~~ Due to the large uncertainty in production

models, hHere we compare the simulated NPP to NPP derived from the three production models aforementioned using MODIS ocean colour estimatesdata.

4.5 Mesozooplankton

MAREDAT, MARine Ecosystem DATA, (Buitenhuis et al., 2013) is a collection of global biomass datasets for major plankton functional types (e.g. diatoms, microzooplankton, mesozooplankton etc.). Mesozooplankton is the only MAREDAT field covering the Indonesian archipelago. The database provides monthly fields at a spatial resolution of 1°. Mesozooplankton data are described in Moriarty and O'Brien (2013). Samples are taken with a single net towed over a fixed depth interval (e.g. 0-50m, 0-100m, 0-150m, 0-200m...) and represent the average population biomass ($\mu\text{g C l}^{-1}$) throughout a depth interval. For this study, only annual mean mesozooplankton biomasses are used. Monthly fields have a too sparse spatial coverage over the Indonesian archipelago and represent different years. It is thus not possible to extract a seasonal cycle.

5 INDO12BIO Evaluation

The ability of the INDO12BIO coupled physical-biogeochemical model to reproduce the observed spatial distribution and temporal variability of biogeochemical tracers is assessed for nutrients and oxygen concentrations, chlorophyll-*a*, ~~net primary production~~ (vertically integrated NPP) and mesozooplankton biomass. Model evaluation focuses on annual mean state, mean seasonal cycle and interannual variability. It is completed by a comparison between model outputs and data from the INDOMIX cruise.

5.1 Annual mean state

5.1.1 Nutrients and Oxygen

Nitrate and oxygen distributions at 100 m depth are presented on Fig. 2 for CARS, WOA and the model. Dissolved ~~Si-silica~~ has the same distribution as nitrate (not shown). The marked meridional gradient, seen in observations of the Pacific and Indian Oceans, is correctly reproduced by the model. Low nitrate and high oxygen concentrations in the subtropical gyres of the North Pacific and South Indian Oceans are due to Ekman-induced downwelling. Higher

nitrate and lower oxygen concentrations in the equatorial area are associated with upwelling. Maxima nitrate concentrations associated with minima oxygen concentrations are noticeable in the Bay of Bengal and Adaman Sea (north of Sumatra and west of Myanmar). They reflect discharges by major rivers (Brahmaputra, Ganges and other river systems) and associated increase in oxygen demand. Low nitrate and high oxygen concentrations at 100 m depth in the Sulawesi Sea reflect the signature of Pacific waters entering in the archipelago, a feature correctly reproduced by the model. The signature slowly disappears as waters progressively mix along their pathways across the archipelago. The resulting higher nitrate and lower oxygen levels at 100 m depth in the Banda Sea are reproduced by the model. Higher nitrate and lower oxygen concentrations off the Java-Nusa-Tenggara island chain in data and model outputs reflect seasonal alongshore upwelling.

To evaluate the vertical distribution of simulated nutrient and oxygen concentrations over the Indonesian archipelago, vertical profiles of oxygen, nitrate and dissolved Si-silica are compared to climatologies provided by CARS and WOA, as well as to discreet data from WOD (Fig. 3). Vertical profiles are analysed in key areas for the Indonesian ThroughFlow (Koch-Larrouy et al., 2007): (1) one box in the North Pacific Ocean, which is representative of water masses entering the archipelago, (2) one box in the Banda Sea where Pacific waters are mixed to form the ITF, and (3) one box at the exit of the Indonesian archipelago (Timor Strait). Biogeochemical characteristics of tropical Pacific water masses entering the archipelago are correctly reproduced by the model (Fig. 3). The flow across the Indonesian archipelago and the transformation of water masses simulated by the model result in realistic vertical distributions of nutrients and oxygen concentrations in the Banda Sea. The ITF leaves the archipelago and spreads into the Indian Ocean with a biogeochemical content in good agreement with the data available in the area.

However, simulated vertical structures are slightly smoothed compared to data (Fig. 3). The vertical gradient of nitrate is too weak over the first 2000m depth of the water column (North Pacific and Timor), and the area of minima oxygen concentrations is eroded (especially in North Pacific box). This bias is even more pronounced on the vertical gradient of dissolved Si-silica (Fig. 3). The smoothing of vertical structures results from the numerical advection scheme MUSCL currently used in PISCES, which is known to be too diffusive (Lévy et al., 2001).

5.1.2 Chlorophyll-*a* and NPP

The simulation reproduces the main characteristics of the large scale distribution of chlorophyll-*a*, a proxy of phytoplankton biomass (Fig. 4). Pacific and Indian subtropical gyres are characterized by low concentrations due to gyre-scale downwelling and hence a deeper nutricline. Highest concentrations are simulated along the coasts driven by riverine nutrient supply, sedimentary processes, as well as upwelling of nutrient-rich deep waters. In comparison to the Case-1 ocean colour product, the model overestimates the chlorophyll-*a* content on oligotrophic gyres and the cross-shore gradient is too weak. As a result, the mean chlorophyll-*a* concentration over the INDO12BIO domain is higher in the simulation ($0.53 \text{ mg Chl m}^{-3}$ with a spatial standard deviation of $0.92 \text{ mg Chl m}^{-3}$ over the domain) compared to MODIS ($0.3 \pm 0.74 \text{ mg Chl m}^{-3}$). The bias (as model – observation) is almost positive everywhere, except around the coasts (discussed later) and in the Sulawesi Sea. As mentioned in the preceding section, optical characteristics of waters over the Indonesian archipelago are closer to Case-2 waters (Moore et al., 2009). Simulated chlorophyll-*a* concentrations are indeed closer to those derived with an algorithm for Case-2 waters (MERIS) and its mean value of $0.48 \pm 1.4 \text{ mg Chl m}^{-3}$.

The model reproduces the spatial distribution, as well the rates of NPP over the model domain (Fig. 5). However, as mentioned before, NPP estimates depend on the primary production model (in this case, VGPM, CbPM, and Eppley) and on the ocean colour data used in the production models. For a single ocean colour product (here MODIS), NPP estimates display a large variability (Fig. 5). Mean NPP over the INDO12BIO domain is $34.5 \text{ mmol C m}^{-2} \text{ d}^{-1}$ for VGPM with a standard deviation over the domain of $33.8 \text{ mmol C m}^{-2} \text{ d}^{-1}$, $40.4 \pm 22 \text{ mmol C m}^{-2} \text{ d}^{-1}$ for CbPM and $55 \pm 52.7 \text{ mmol C m}^{-2} \text{ d}^{-1}$ for Eppley. NPP estimates from VGPM are characterized by low rates in the Pacific ($<10 \text{ mmol C m}^{-2} \text{ d}^{-1}$) and a well marked cross-shore gradient. The use of CbPM results in low coastal NPP and almost uniform rates over a major part of the domain and including the open ocean (Fig. 5). The Eppley production model is the most productive one with rates about $15 \text{ mmol C m}^{-2} \text{ d}^{-1}$ in the Pacific and higher than $300 \text{ mmol C m}^{-2} \text{ d}^{-1}$ in the coastal zone. The large uncertainty associated with these products precludes a quantitative evaluation of modelled NPP. Like for chlorophyll-*a*, modelled NPP falls within the range of remote sensing derived estimates, with maybe a too weak cross-shore

gradient inherited from the chlorophyll-*a* field. The mean NPP over the INDO12BIO domain is, however, overestimated ($61 \pm 41.8 \text{ mmol C m}^{-2} \text{ d}^{-1}$).

5.1.3 Mesozooplankton

Mesozooplankton links the first level of the marine food web (primary producers) to the mid- and, ultimately, high trophic levels. Modelled mesozooplankton biomass is compared to observations in Fig. 6. While the model reproduces the spatial distribution of mesozooplankton, it overestimates biomass by a factor 2 or 3. This overestimation is likely linked to the above-described overestimation of chlorophyll-*a* and NPP.

5.2 Mean seasonal cycle

The monsoon system drives the seasonal variability of chlorophyll-*a* over the area of study. Northern and southern parts of the archipelago exhibit a distinct seasonal cycle (Fig. 7, 8 and 9). In the southern part, the highest chlorophyll-*a* concentrations occur from June to September (Banda Sea and Sunda area in Fig. 8 and 9) due to upwelling of nutrient-rich waters off Sunda Islands and in the Banda Sea triggered by alongshore south-easterly winds during SE monsoon. The decrease in chlorophyll levels during NW monsoon is the consequence of north-westerly winds and associated downwelling in these same areas. In the northern part, high chlorophyll concentrations occur during NW monsoon (South China Sea in Fig. 7) when moist winds from Asia cause intense precipitations. A secondary peak is observed during NW monsoon in the southern part and during SE monsoon in the northern part due to meteorological and oceanographic conditions described above.

The annual signal of chlorophyll-*a* in each grid point gives a synoptic view of the effect of the Asia-Australia monsoon system on the Indonesian archipelago. A harmonic analysis is applied on the time series of each grid point to extract the annual signal in model output and remote sensing data (MODIS). The results of the annual harmonic analysis are summarized in Fig. 10 and highlight the month of maximum chlorophyll-*a* and the amplitude of the annual signal. The timing of maximum chlorophyll-*a* presents a north-south distribution in agreement with the satellite observations. The simulation reproduces the chlorophyll-*a* maxima in July in the Banda Sea and off the south coasts of Java-Nusa-Tenggara. Consistent with observations, simulated chlorophyll-*a* maxima move to the west over the period of the SE monsoon, in

response to the alongshore wind shift. North of the Nusa-Tenggara Islands, maxima in January-February are due to upwelling associated with alongshore north-westerly winds. In the South China Sea, maxima spread from July-August in the western part (off Mekong River) and gradually shift up to January-February in the eastern part.

The temporal correlation between modelled chlorophyll-*a* and estimates derived from remote sensing is 0.55 over the entire INDO12BIO domain, but reaches 0.78 in the South China Sea, 0.81 in the Banda Sea and 0.932 in the Indian Ocean (Fig. 7, 8, 9 and 11). These high correlation coefficients are associated with low normalized standard deviations (close to 1) in the Banda Sea and in the Indian Ocean (Fig. 11) and large amplitudes in simulated and observed chlorophyll-*a* (Fig. 10). Normalized standard deviations are higher in the South-East China Sea, Java and Flores Seas, but also in the open ocean due to larger amplitudes in simulated chlorophyll-*a*. The offshore spread of the high amplitude reflects the too weak cross-shore gradient of simulated chlorophyll-*a* (Section 5.1.2), and leads to an increase of the normalized standard deviation with the distance to the coast. For semi-enclosed seas, however, this result has to be taken with caution as clouds cover these regions almost 50-60% of the time period.

The model does not succeed in simulating chlorophyll-*a* variability in the Pacific sector (Fig. 10 and 11). This area is close to the border of the modelled domain and is influenced by the OBCs derived from the global operational ocean general circulation model. Analysis of the modelled circulation (Part 1) highlights the role of OBCs in maintaining realistic circulation patterns in this area, which is influenced by the equatorial current system. Part 1 points, in particular, to the incorrect positioning of Halmahera and Mindanao eddies in the current model, which contributes to biases in simulated biogeochemical fields.

Finally, correlation is low close to the coasts and the temporal variability of the model is lower than that of the satellite product, with normalized standard deviation < 1 (Fig. 11). The model does not take into account seasonal ~~variable nutrient input from rivers~~variations in river discharges. D-driven by the monsoon system, seasonal input of river runoff.~~The seasonality of external sources of nutrients~~ is an important driver of chlorophyll-*a* variability at local scale.

5.3 Interannual variability

Figures 7, 8 and 9 present interannual anomalies of surface chlorophyll-*a* concentrations between 2008 and 2014 for model outputs and MODIS ocean colour averaged over three regions: South China Sea, Banda Sea and Sunda area. Simulated fields and satellite-derived chlorophyll-*a* are in good agreement in terms of amplitude and phasing, with temporal correlation coefficients of 0.56 for South China Sea and Banda Sea and 0.878 for Sunda area. The model simulates a realistic temporal variability suggesting that processes regulating the seasonal as well as interannual variability of the Indonesian region are correctly reproduced. While the mean seasonal cycle of chlorophyll-*a* is driven by the strength and timing of the ~~seasonal~~ Asian monsoon, anomalies are driven by interannual climate modes, such as El Niño Southern Oscillation (ENSO) and Indian Ocean Dipole (IOD).

IOD drives the chlorophyll-*a* interannual variability in the Eastern Tropical Indian Ocean, with a correlation coefficient of 0.74 (Fig. 9). IOD index and anomalies of chlorophyll-*a* from satellite give a similar correlation coefficient of 0.7. A positive phase of IOD indicates negative SST anomaly in the South-Eastern Tropical Indian Ocean associated with zonal wind anomaly along the equator (Meyers, 1996). The abnormally strong coastal upwelling near the Java Island stimulates a large phytoplankton bloom (Murtugudde et al., 1999). In the Banda Sea and in the South China Sea, no clear impact of ENSO or IOD is detected on the first level of the food chain (Fig. 7, 8). Inside the archipelago, both climate modes affect the variability of the ITF transport and it is not straightforward to separate their individual contribution (Masumoto, 2002; Sprintall and Révelard, 2014).

While it is established (see references cited in Section 2) that ENSO and IOD climate modes play a key role in the Indonesian region, their impact on the marine ecosystem remains poorly understood. The length of simulation is too short for a rigorous assessment of the role of these drivers and a direct relationship is only evident in the Indian sector. However, interannual anomalies of simulated chlorophyll-*a* compare well to satellite observations, which suggests that interannual meteorological and ocean physical processes are satisfyingly reproduced by the model.

5.4 INDOMIX cruise

Model results are compared to INDOMIX *in-situ* data at three key locations: (1) the eastern entrance of Pacific waters to the archipelago (station 3, Halmahera Sea), (2) the convergence of the western and eastern pathways (station 4, Banda Sea) where intense tidal mixing and upwelling transforms Pacific waters to form the ITF, and (3) one of the main exit portals of the ITF to the Indian Ocean (station 5, Ombai Strait).

The vertical profile of temperature compares well to the data in the Halmahera Sea (Fig. 12). Simulated surface waters are too salty and the subsurface salinity maximum is reproduced at the observed depth, albeit underestimated compared to the data. Waters are more oxygenated in the model over the first 400 m. The model-data bias on temperature, salinity and oxygen suggests that Halmahera Sea thermocline waters are not correctly reproduced by the model in July 2010. The model tends to yield too smooth vertical profiles. Vertical profiles of nitrate and phosphate are well reproduced, while dissolved ~~Si-silica~~ concentrations are overestimated below 200 m depth. It should be noted, however, that 2010 was a strong La Niña year with important modifications in zonal winds, rainfall, river discharges and ocean currents. While interannual variability is taken into account in atmospheric forcing and physical open boundary conditions, ~~this is not the case for biogeochemistry.~~ External nutrient inputs from rivers are constant, and ~~biogeochemical OBCs open boundary conditions~~ come from ~~monthly~~ climatologies. ~~However, d~~Dissolved ~~Si-silica~~ profiles computed from the monthly WOA2009 climatology are close to simulated distributions (not shown), suggesting non-standard conditions during the time of the INDOMIX cruise.

Despite the bias highlighted for Halmahera Sea station, an overall satisfying correspondence between modelled and observed profiles is found at the Banda Sea (Fig. 13) and Ombai Strait stations (Fig. 14). The comparison of modelled profiles and cruise data along the flow path of waters from the Pacific to the Indian Ocean (from Halmahera to Ombai Strait) suggests that either the Halmahera Sea had no major influence for the ITF formation during the time of the cruise, or that vertical mixing and upwelling processes across the archipelago are strong enough to allow the formation of Indonesian water masses despite biases in source water composition. Alternatively, it could reflect the weak impact of ENSO on biogeochemical tracer distributions inside the archipelago compared to its Pacific border and the dominant role of Indian ocean dynamics on the ITF (Sprintall and Révelard, 2014).

6 Discussions and conclusions

The INDES0 project aims to monitor and forecast marine ecosystem dynamics in Indonesian waters. A suite of numerical models ~~has been~~ were coupled for setting up a regional configuration (INDO12) adapted to Indonesian seas. A forecasting oceanographic centre is fully operational in Perancak (Bali, Indonesia) since mid-September 2014. Here we ~~access~~ assess the skill of the ~~OPA-NEMO-OPA~~ hydrodynamical model coupled to the PISCES biogeochemical model (INDO12BIO configuration). A 8-year long hindcast simulation was launched starting in January 2007 and has caught up with real time. ~~The strengths of the simulation are reminded below and weaknesses are discussed as follow: coastal ocean, cross-shore gradient and open ocean. In the following paragraphs, the strengths of the simulation are first reviewed and weaknesses are then discussed.~~

The large scale distribution of nutrient, oxygen, chlorophyll-*a*, NPP and mesozooplankton biomass are well reproduced. The vertical distribution of nutrient and oxygen is comparable to *in-situ* based datasets. Biogeochemical characteristics of North Pacific tropical waters entering in the archipelago are set by the open boundaries. The transformation of water masses by hydrodynamics across the Indonesian archipelago is satisfyingly simulated. As a result, nitrate and oxygen vertical distributions match observations in Banda Sea and at the exit of the archipelago. The seasonal cycle of surface chlorophyll-*a* is in phase with satellite estimations. The northern and southern parts of the archipelago present a distinct seasonal cycle, with higher chlorophyll concentrations in the southern part during SE monsoon, and in the northern part of the archipelago during NW monsoon. The interannual variability of surface chlorophyll-*a* correlates with satellite observations in several regions (South China Sea, Banda Sea and Indian part); this. ~~These anomalies~~ suggests that meteorological and ocean physical processes that drive the interannual variability in the Indonesian region are correctly reproduced by the model. The relative contribution of ENSO and IOD interannual climate modes to the interannual variability of chlorophyll-*a* is still an open question, and will be ~~deepened in a future study~~ further investigated.

However, ~~m~~Mean chlorophyll-*a* ($0.53 \text{ mg Chl m}^{-3}$) and NPP ($61 \text{ mmol C m}^{-2} \text{ d}^{-1}$) are systematically overestimated. Around the coasts, the temporal correlation between simulated

chlorophyll-*a* and satellite data breaks down. Simulated vertical profiles of nutrient and oxygen are too diffusive as compared to data.

In coastal waters, chlorophyll-*a* concentrations are influenced by sedimentary processes (i.e. remineralization of organic carbon and subsequent release of nutrients) and riverine nutrient input. The slight disequilibrium explicitly introduced between the external input of nutrients and carbon and the loss to the sediment is sufficient to enhance chlorophyll-*a* concentrations along the coasts and to make it comparable with observations~~in line with observations~~. The sensitivity of the model to the balancing of carbon and nutrients at the lower boundary of the domain (“sediment burial”) highlights the need for an explicit representation of sedimentary reactions.

In order to further improve modelled chlorophyll-*a* variability along the coast, time-variant river nutrient and carbon fluxes will be needed. According to Jennerjahn et al. (2004), river discharges from Java can be increased by a factor of ~12 during NW monsoon as compared to SE monsoon. Moreover the maximum fresh water transport and the peak of material reaching the sea can be out of phase depending on the origin of discharged material (Hendiarti et al., 2004). The improved representation of river discharge dynamics and associated delivery of fresh water, nutrients and suspended matter in the model is, however, hampered by the availability of data as~~most~~ of the Indonesian rivers are currently not monitored (Susanto et al., 2006).

Systematic misfits between modelled and observed biogeochemical distributions may in part also reflect inherent properties of implemented numerical schemes. Misfits highlighted throughout this work include too much chlorophyll-*a* and NPP on the shelves, with too weak cross-shore gradients between shelf and open waters, together with noticeable smoothing of vertical profiles of nutrients and oxygen. Currently, the MUSCL advection scheme is used for biogeochemical tracers. This scheme is too diffusive and smooths vertical profiles of biogeochemical tracers. As a result, too much nutrients are injected in the surface layer and trigger high levels of chlorophyll-*a* and NPP. Another advection scheme, QUICKEST (Leonard, 1979) with the limiter of Zalezak (1979), already used in NEMO for the advection scheme of the physical model, has been tested for biogeochemical tracers. Switching from MUSCL to QUICKEST-Zalezak accentuates the vertical gradient of nutrients in the water column and attenuates modelled chlorophyll-*a* and NPP. This advection scheme is not

diffusive and its use would be coherent with choices adopted for physical tracers. ~~However, it results in an overestimation of the vertical gradient of nutrients, and the nutricline is considerably strengthened.~~ However, it would result in an overestimation of the vertical gradient of nutrients, and the nutricline would be considerably strengthened. Neither tuning of biogeochemical parameters, nor switching the advection scheme for passive tracers fully resolved the model-data misfits. Hence iImproving the vertical distribution of nutrients and oxygen, as well as chlorophyll-*a* and NPP in the open ocean and their cross-shore gradient first requires improving the model physics~~relies at first order on the model physics.~~

Finally, monthly or yearly climatologies are currently used for initial and open boundary conditions. Biogeochemical tracers are thus decorrelated from model physics. In order to improve the link between modelled physics and biogeochemistry, weekly or monthly averaged output of the global ocean operational system operated by Mercator Ocean (BIOMER) will be used in the future for the 24 tracers of the biogeochemical model PISCES. BIOMER will couple the physical forecasting system PSY3 to PISCES in off-line mode. The biogeochemical and the physical components of INDOBIO12 will thus be initialized and forced coherently, on the base of the ~~by the same~~ PSY3 forecasting system.

Code and Data Availability

The INDO12 configuration is based on the NEMO 2.3 version developed by the NEMO consortium. All specificities included in the NEMO code version 2.3 are now freely available in the recent version NEMO 3.6 (<http://www.nemo-ocean.eu>). The biogeochemical model PISCES is coupled to hydrodynamic model by the TOP component of the NEMO system. PISCES 3.2 and its external forcing are also available via the NEMO web site. World Ocean Database and World ocean Atlas are available at <https://www.nodc.noaa.gov>. Glodap data are available at <http://cdiac.ornl.gov/oceans/glodap/GlopDV.html>. MODIS and MERIS ocean colour products are respectively available at <http://oceancolor.gsfc.nasa.gov/cms/> and <http://hermes.acri.fr/>, Primary production estimates based on VGPM, Eppley and CbPM algorithms at http://www.science.oregonstate.edu/ocean_productivity/.

Acknowledgements

The authors acknowledge financial support through the INDES0 (01/Balitbang KP.3/INDES0/11/2012) and Mercator Vert (LEFE/GMMC) projects. They thank Christian Ethé for its technical advice on NEMO-OPA/PISCES. Ariane Koch-Larrouy provided INDOMIX data. We also thank our colleagues of Mercator Ocean and CLS for their contribution to the model evaluation (Bruno Levier, Clément Bricaud, Julien Paul) and especially Eric Greiner for his useful recommendations and advice on the manuscript.

References

- Allen, G. R.: Conservation hotspots of biodiversity and endemism for Indo-Pacific coral reef fishes, *Aquatic Conserv: Mar. Freshw. Ecosyst.*, 18: 541–556, doi:10.1002/aqc.880, 2008.
- Allen, G. R., and Werner, T. B.: Coral Reef Fish Assessment in the ‘Coral Triangle’ of Southeastern Asia, *Environmental Biology of Fishes*, 65(2), 209-214, doi:10.1023/A:1020093012502, 2002.
- Alongi, D. A., da Silva, M., Wasson, R. J., and Wirasantosa, S.: Sediment discharge and export of fluvial carbon and nutrients into the Arafura and Timor Seas: A regional synthesis, *Marine Geology*, 343, 146–158, doi:10.1016/j.margeo.2013.07.004, 2013.
- Aumont, O., and Bopp, L.: Globalizing results from ocean in situ iron fertilization studies, *Global Biogeochem. Cycles*, 20, GB2017, doi:10.1029/2005GB002591, 2006.
- Aumont, O., Maier-Reimer, E., Blain, S., and Monfray, P.: An ecosystem model of the global ocean including Fe, Si, P colimitations. *Global Biogeochem. Cycles*, 17(2), 1060, doi:10.1029/2001GB001745, 2003.
- Ayers, J. M., Strutton, P. G., Coles, V. J., Hood, R. R., and Matear, R. J.: Indonesian throughflow nutrient fluxes and their potential impact on Indian Ocean productivity, *Geophys. Res. Lett.*, 41(14), 5060-5067, doi:10.1002/2014GL060593, 2014.
- Behrenfeld, M. J., and Falkowski, P. G.: Photosynthetic rates derived from satellite-based chlorophyll concentration, *Limnol. Oceanogr.*, 42(1), 1-20, 1997.
- Behrenfeld, M. J., Boss, E., Siegel, D. A., and Shea, D. M.: Carbon-based ocean productivity and phytoplankton physiology from space, *Global Biogeochem. Cycles*, 19(1), GB1006, doi:10.1029/2004GB002299, 2005.
- Bryant, D., Burke, L., McManus, J., and Spalding, M.: *Reefs at Risk: A Map-Based Indicator of Potential Threats to the World’s Coral Reefs*, World Resources Institute, Washington, DC; International Center for Living Aquatic Resource Management, Manila; and United Nations Environment Programme–World Conservation Monitoring Centre, Cambridge, 1998.
- Buitenhuis, E. T., Vogt, M., Moriarty, R., Bednaršek, N., Doney, S. C., Leblanc, K., Le Quéré, C., Luo, Y.-W., O'Brien, C., O'Brien, T., Peloquin, J., Schiebel, R., and Swan, C.:

MAREDAT: towards a world atlas of MARine Ecosystem DATA, *Earth Syst. Sci. Data*, 5, 227-239, doi:10.5194/essd-5-227-2013, 2013.

Cros, A., Fatan, N. A. White, A., Teoh S. J., Tan, S., Handayani, C., Huang, C., Peterson, N., Li, R. V., Siry, H. Y., Fitriana, R., Gove, J., Acoba, T., Knight, M., Acosta, R., Andrew, N., and Beare, D.: The Coral Triangle Atlas: An Integrated Online Spatial Database System for Improving Coral Reef Management, *PLoS ONE* 9(6): e96332. doi:10.1371/journal.pone.0096332, 2014.

CSIRO: Atlas of Regional Seas, available at: <http://www.marine.csiro.au/~dunn/cars2009/> (last access: 13 August 2015), 2009.

Doerffer, R. and Schiller, H: The MERIS Case 2 water algorithm, *International Journal of Remote Sensing*, 28, 517-535, doi:10.1080/01431160600821127, 2007.

FAO: United Nations Food and Agricultural Organization, FAOSTAT, available at: <http://faostat.fao.org/site/291/default.aspx> (last access: 13 August 2015), 2007.

Ffield, A., and Gordon, A. L.: Vertical Mixing in the Indonesian Thermocline, *J. Phys. Oceanogr.*, 22, 184-195, 1992.

Ffield, A., and Gordon, A. L.: Tidal mixing signatures in the Indonesian Seas. *J. Phys. Oceanogr.*, 26, 1924–1937, 1996.

Foale, S., Adhuri, D., Aliño, P., Allison, E. H., Andrew, N., Cohen, P., Evans, L., Fabinyi, M., Fidelman, P., Gregory, C., Stacey, N., Tanzer, J., and Weeratunge, N.: Food security and the Coral Triangle Initiative, *Marine Policy*, 38, 174-183, doi:10.1016/j.marpol.2012.05.033, 2013.

Garcia, H. E., Locarnini, R. A., Boyer, T. P., Antonov, J. I., Baranova, O. K., Zweng, M. M., and Johnson, D. R.: World Ocean Atlas 2009, Volume 3: Dissolved Oxygen, Apparent Oxygen Utilization, and Oxygen Saturation. S. Levitus, Ed. NOAA Atlas NESDIS 70, U.S. Government Printing Office, Washington, D.C., 344 pp., 2010a.

Garcia, H. E., Locarnini, R. A., Boyer, T. P., Antonov, J. I., Zweng, M. M., Baranova, O. K., and Johnson, D. R.: World Ocean Atlas 2009, Volume 4: Nutrients (phosphate, nitrate, silicate). S. Levitus, Ed. NOAA Atlas NESDIS 71, U.S. Government Printing Office, Washington, D.C., 398 pp., 2010b.

- Ginsburg, R. N.: Ed., Proceedings of the Colloquium on Global Aspects of Coral Reefs: Health, Hazards and History, Atlantic Reef Committee, 1994.
- Gordon, A. L.: Oceanography of the Indonesian seas and their throughflow, *Oceanography*, 18(4), 14–27, doi:10.5670/oceanog.2005.01, 2005.
- Green, A., and Mous, P. J.: Delineating the Coral Triangle, its ecoregions and functional seascapes. Report on an expert workshop held in Southeast Asia Center for Marine Protected Areas, Bali, Indonesia, April 30-May 2, 2003, The Nature Conservancy, 2004.
- Hendiarti, N., Siegel, H., and Ohde, T.: Investigation of different coastal processes in Indonesian waters using SeaWiFS data, *Deep-Sea Research Part II*, 51(1-3), 85-97, doi:10.1016/j.dsr2.2003.10.003, 2004.
- Hendiarti, N., Suwarso, E., Aldrian, E., Amri, K., Andiastuti, R., Sachoemar, S. I., and Wahyono, I. B.: Seasonal variation of pelagic fish catch around Java, *Oceanography*, 18(4), 112-123, doi:10.5670/oceanog.2005.12, 2005.
- Henson, S. A., Sarmiento, J. L., Dunne, J. P., Bopp, L., Lima, I., Doney, S. C., John, J., and Beaulieu, C.: Detection of anthropogenic climate change in satellite records of ocean chlorophyll and productivity, *Biogeosciences*, 7(2), 621–640, doi:10.5194/bg-7-621-2010, 2010.
- Hirst, A. C., and Godfrey, J. S.: The role of Indonesian ThroughFlow in a global ocean GCM, *J. Phys. Oceanogr.*, 23(6), 1057–1086, 1993.
- Hopley, D. and Suharsono, M.: *The Status of Coral Reefs in Eastern Indonesia*. Australian Institute of Marine Science, Townsville, Australia, 2000.
- Jennerjahn, T. C., Ittekkot, V., Klopper, S., Adi, S., Purwo Nugroho, S., Sudiana, N., Yusmal, A., and Gaye-Haake, B.: Biogeochemistry of a tropical river affected by human activities in its catchment: Brantas River estuary and coastal waters of Madura Strait, Java, Indonesia, *Estuarine Coastal Shelf Sci.*, 60(3), 503–514, doi:10.1016/j.ecss.2004.02.008, 2004.
- Key, R. M., Kozyr, A., Sabine, C. L., Lee, K., Wanninkhof, R., Bullister, J., Feely, R.A., Millero, F., Mordy, C. and Peng, T.-H.: A global ocean carbon climatology: Results from GLODAP. *Global Biogeochemical Cycles*, Vol. 18, GB4031, 2004.

- Koch-Larrouy, A., Madec, G., Bouruet-Aubertot, P., Gerkema, T., Bessieres, L., and Molcard, R.: On the transformation of Pacific Water into Indonesian Throughflow Water by internal tidal mixing, *Geophys. Res. Lett.*, 34, L04604, doi:10.1029/2006GL028405, 2007.
- Koch-Larrouy, A., Morrow, R., Penduff, T., and Juza, M.: Origin and mechanism of Subantarctic Mode Water formation and transformation in the Southern Indian Ocean, *Ocean Dynamics*, 60(3), 563-583, doi:10.1007/s10236-010-0276-4, 2010.
- Koch-Larrouy, A., Atmadipoera, A., Van Beek, P., Madec, G., Aucan, J., Lyard, F., Grelet, J. and Souhaut, M.: Estimates of tidal mixing in the Indonesian archipelago from multidisciplinary INDOMIX in-situ data, *Deep Sea Research part 1*, M DSR1-D-14-00245R1, in revision, 2015.
- Lehodey, P., Senina, I., and Murtugudde, R.: A spatial ecosystem and populations dynamics model (SEAPODYM) – Modeling of tuna and tuna-like populations, *Progress in Oceanography*, 78, 304–318, 2008.
- Leonard, B. P.: A stable and accurate convective modelling procedure based on quadratic upstream interpolation, *Comp. Method. Appl. M.* 19, 59–98, 1979.
- Lévy, M., Estublier, A., and Madec, G.: Choice of an Advection Scheme for Biogeochemical Models, *Geophysical Research Letters*, 28(19), 3725-3728, 2001.
- Ludwig, W., Probst, J. L., and Kempe, S.: Predicting the oceanic input of organic carbon by continental erosion, *Global Biogeochem.Cycles*, 10(1), 23– 41, doi:10.1029/95GB02925, 1996.
- Madden, R. A., and Julian P. R.: Observations of the 40–50 day tropical oscillation - A review, *Monthly Weather Reviews*, 122(5), 814–837, 1994.
- Madec G.: "NEMO ocean engine", Note du Pole de modélisation, Institut Pierre-Simon Laplace (IPSL), France, No 27 ISSN No 1288-1619, 2008.
- Madec, G., Delecluse, P., Imbard, M., and Lévy, C.: "OPA 8.1 Ocean General Circulation Model reference manual", Note du Pole de modélisation, Institut Pierre-Simon Laplace (IPSL), France, No11, 91pp., 1998.
- Masumoto, Y.: Effects of Interannual Variability in the Eastern Indian Ocean on the Indonesian Throughflow, *Journal of Oceanography*, 58, 175-182, 2002.

- Meyers, G.: Variation of Indonesian throughflow and the El Niño-Southern Oscillation. *J. Geophys. Res.*, 101, 12,475–12,482, 1996.
- Milliman, J. D., Farnsworth, K. L., and Albertin, C. S.: Flux and fate of fluvial sediments leaving large islands in the East Indies, *J. Sea Res.*, 41(1-2), 97–107, 1999.
- Moore, T. S., Campbell, J. W., and Dowell, M. D: A class-based approach to characterizing and mapping the uncertainty of the MODIS ocean chlorophyll product, *Remote Sensing of Environment*, 113, 2424-2430, 2009.
- Mora, C., Chittaro, P. M., Sale, P. F., Kritzer, J. P., and Ludsin, S.A.: Patterns and processes in reef fish diversity, *Nature*, 421, 933-936, doi:10.1038/nature01393, 2003.
- Moriarty, R., and O'Brien, T. D.: Distribution of mesozooplankton biomass in the global ocean, *Earth System Science Data*, 5,45-55, 2013.
- Murtugudde, R., Busalacchi, A. J., and Beauchamp, J.: Seasonal-to-interannual effects of the Indonesian Throughflow on the tropical Indo-Pacific Basin. *J. Geophys. Res.*, 103, 21,425–21,441, 1998.
- Murtugudde, R., Signorini, S. R., Christian, J. R., Busalacchi, A. J., McClain, C. R., and Picaut, J.: Ocean color variability of the tropical Indo-Pacific basin observed by SeaWiFS during 1997–1998. *J. Geophys. Res.*, 104, 18,351–18,366, 1999.
- Pimentel D., Harvey, C., Resosudarmo, P., Sinclair, K., Kurz, D., McNair, M., Crist, C., Shpritz, L., Fitton, L., Saffouri, R., and Blair, R.: Environmental and Economic Costs of Soil Erosion and Conservation Benefits, *Science*, 267(5201), 1117-1123, 1995.
- Potemra, J. T., Lukas, R., and Mitchum, G. T.: Large-scale estimation of transport from the Pacific to the Indian Ocean. *J. Geophys. Res.*, 102, 27,795–27,812, 1997.
- Rixen, T., Ittekkot, V., Herunadi, B., Wetzel, P., Maier-Reimer, E., and Gaye-Haake, B.: ENSO-driven carbon sea saw in the Indo-Pacific, *Geophys. Res. Lett.*, 33, L07606, doi:10.1029/2005GL024965, 2006.
- Roberts, C. M., McClean, C. J., Veron, J. E. N., Hawkins, J. P., Allen, G. R., McAllister, D. E., Mittermeier, C. G., Schueler, F. W., Spalding, M., Wells, F., Vynne, C., and Werner, T. B.: Marine Biodiversity Hotspots and Conservation Priorities for Tropical Reefs, *Science*, 295(5558), 1280-1284, doi10.1126/science.1067728, 2002.

Romero, O. E., Rixen, T., and Herunadi, B.: Effects of hydrographic and climatic forcing on diatom production and export in the tropical southeastern Indian Ocean, *Mar. Ecol. Prog. Ser.*, 384, 69-82, doi:10.3354/meps08013, 2009.

Saji, N. H., Goswami, B. N., Vinayachandran, P. N., and Yamagata, T.: A dipole mode in the tropical Indian Ocean. *Nature*, 401, 360–363, 1999.

Sprintall, J., Gordon, A. L., Murtugudde, R., and Susanto, R. D.: A semi-annual Indian Ocean forced Kelvin waves observed in the Indonesian Seas, May 1997. *J. Geophys. Res.*, 105(C7), 17217–17230, doi:10.1029/2000JC900065, 2000.

Sprintall, J., and Révelard, A.: The Indonesian throughflow response to Indo-Pacific climate variability, *J. Geophys. Res. Oceans*, 119, 1161–1175, doi:10.1002/2013JC009533, 2014.

Susanto, R. D., and Marra, J.: Effect of the 1997/98 El Niño on chlorophyll a variability along the southern coasts of Java and Sumatra, *Oceanography*, 18(4), 124–127, doi:10.5670/oceanog.2005.13, 2005.

Susanto, R. D., Gordon, A. L., Sprintall, J., and Herunadi, B.: Intraseasonal variability and tides in Makassar Strait. *Geophys. Res. Lett.*, 27, 1499–1502, 2000.

Susanto, R. D., Gordon, A. L., and Zheng, Q.: Upwelling along the coasts of Java and Sumatra and its relation to ENSO, *Geophys. Res. Lett.*, 28(8), 1599-1602, doi:10.1029/2000GL011844, 2001.

Susanto, R. D., Moore, T. S., and Marra, J.: Ocean color variability in the Indonesian Seas during the SeaWiFS era, *Geochemistry Geophysics Geosystems*, 7(5), Q05021, doi:10.1029/2005GC001009, 2006.

Tegen, I., and Fung, I.: Contribution to the Atmospheric Mineral Aerosol Load From Land-Surface Modification, *J Geophys Res-Atmos*, 100, 18707–18726, 1995.

~~Tranchant, B., Reffray, G., Greiner, E., Nugroho, D., Koch-Larrouy, A., and Gaspar, P.: Evaluation of an operational ocean model configuration at 1/12° spatial resolution for the Indonesian seas. Part I: ocean physics, *Geosci. Model Dev. Discuss.*, 8, 6611–6668, doi:10.5194/gmdd-8-6611-2015, 2015.~~
Tranchant, B., Reffray, G., Greiner, E., Nugroho, D., Koch-Larrouy, A., and Gaspar, P.: Evaluation of an operational ocean model configuration at

[1/12° spatial resolution for the Indonesian seas \(NEMO2.3/INDO12\) – Part 1: Ocean physics, Geosci. Model Dev., 9, 1037-1064, doi:10.5194/gmd-9-1037-2016, 2016.](#)

UNEP: Vantier, L., Wilkinson, C., Lawrence, D. and Souter, D. (Eds.): Indonesian Seas, GIWA Regional Assessment 57, University of Kalmar, Kalmar, Sweden, 2005.

UNEP: Sherman, K. and Hempel, G. (Eds.): The UNEP Large Marine Ecosystem Report: A perspective on changing conditions in LMEs of the world's Regional Seas, United Nations Environment Programme. Nairobi, Kenya, 2009.

Van Leer, B.: Towards the Ultimate Conservative Difference Scheme. IV. A New Approach to Numerical Convection, *J. Comput. Phys.*, 23, 276-299, 1977.

Veron, J. E. E., Devantier, L. M., Turak, E., Green, A. L., Kininmonth, S., Stafford-Smith, M., and Peterson, N.: Delineating the Coral Triangle, *Galaxea, J. Coral Reef Studies* 11, 91-100, 2009.

Westberry, T., Behrenfeld, M. J., Siegel, D. A., and Boss, E.: Carbon-based primary productivity modeling with vertically resolved photoacclimation, *Global Biogeochem. Cycles*, 22(2), GB2024, doi:10.1029/2007GB003078, 2008.

WOA: World Ocean Atlas, available at: http://www.nodc.noaa.gov/OC5/WOA09/pr_woa09.html (last access: 13 August 2015), 2009.

WOD: World Ocean Database, available at: http://www.nodc.noaa.gov/OC5/WOD09/pr_wod09.html (last access: 13 August 2015), 2009.

Wolter, K., and Timlin, M. S.: Measuring the strength of ENSO events - how does 1997/98 rank? *Weather*, 53, 315-324, 1998.

Wolter, K., and Timlin, M. S.: El Niño/Southern Oscillation behaviour since 1871 as diagnosed in an extended multivariate ENSO index (MEI.ext). *Intl. J. Climatology*, 31, 1074-1087, 2011.

Zalesak, S. T.: Fully multidimensional flux-corrected transport algorithms for fluids, *J. Computat. Phys.*, 31, 335-362, 1979.

Table caption

Table 1. Initial and open boundary conditions used for the INDO12BIO configuration.

Figure caption

Figure 1. Temporal evolution of total carbon (a), plankton (b), DIC and DOC (c) and nutrient (d, e) content averaged over the whole 3-dimensional INDO12BIO domain.

Figure 2: Annual mean of nitrate (mmol N m^{-3} ; left) and oxygen concentrations ($\text{ml O}_2 \text{ l}^{-1}$; right) at 100 m depth from CARS (a, d) and WOA (b, e; statistical mean) annual climatologies, and from INDO12BIO as 2010-2014 averages (c, f). Three key boxes for water mass transformation (North Pacific, Banda, and Timor; Koch-Larrouy et al., 2007) were added to the bottom-right figure.

Figure 3: Vertical profiles of oxygen ($\text{ml O}_2 \text{ l}^{-1}$; top: a, d, g), nitrate (mmol N m^{-3} ; middle: b, e, h) and dissolved silica (mmol Si m^{-3} ; bottom: c, f, i) in 3 key boxes for water masses transformation (North Pacific, left; Banda, middle; and Timor, right) (see Fig. 2; Koch-Larrouy et al., 2007). CARS and WOA annual climatologies are in red and dark blue. INDO12BIO simulation averaged between 2010 and 2014 is in black. All the raw data available on each box and gathered in the WOD (light blue crosses) are added in order to illustrate the spread of data.

Figure 4. Left) Annual mean of surface chlorophyll-*a* concentrations (mg Chl m^{-3}) for year 2011: MODIS Case-1 product (a), MERIS Case-2 product (b) and INDO12BIO simulation (c). Right) Bias of log-transformed surface chlorophyll (model-observation) for the same year. The model was masked as a function of the observation, MODIS Case-1 (d) or MERIS Case-2 (e). Location of 3 stations sampled during the INDOMIX cruise and used for evaluation of the model in Section 4.4 (f).

Figure 5. Annual mean of vertically integrated ~~primary production~~NPP ($\text{mmol C m}^{-2} \text{ d}^{-1}$) for year 2011: VGPM (a), Eppley (d), and CbPM (b) production models, all based on MODIS ocean colour, as well as for INDO12BIO (e). Standard deviation of the 3 averaged production models (PM) (c), and bias between INDO12BIO and the average of PM (f).

Figure 6: Annual mean of mesozooplankton biomass ($\mu\text{g C l}^{-1}$) from MAREDAT monthly climatology (left) and from INDO12BIO simulation averaged between 2010 and 2014 (right), for distinct depth interval: from the surface up to 40m (a, e), 100m (b, f), 150m (c, g), and 200m depth (d, h). Simulated fields were interpolated onto the MAREDAT grid, and masked as a function of the data (in space and time).

Figure 7: a) Mean surface chlorophyll-*a* concentrations and b) its interannual anomalies (mg Chl m^{-3}) over the South China Sea. INDO12BIO is in black and MODIS Case-1 in red. Temporal correlation (*r*) between both time series is in black. c) ENSO (blue) and IOD (green) phenomena are respectively represented by MEI and DMI indexes. Indexes were normalized by their maximum value in order to be plotted on the same axis. Interannual anomalies of simulated chlorophyll-*a* are reminded in black. Temporal correlation (*r*) between the simulated chlorophyll-*a* and ENSO (IOD) is indicated in blue (green).

Figure 8: Same as Figure 7, in Banda Sea.

Figure 9: Same as Figure 7, in Sunda area.

Figure 10. Timing of maximum chlorophyll-*a* (a, c) and amplitude (b, d) for a monthly climatology of surface chlorophyll-*a* concentrations between 2010 and 2014: MODIS Case-1 (left) and INDO12BIO (right). The model was masked as a function of the data.

Figure 11: Temporal correlation (a) and normalised standard deviation ($\text{std}(\text{model})/\text{std}(\text{data})$) estimated between the INDO12BIO simulation and the MODIS Case-1 ocean colour product. Statistics are computed on monthly fields between 2010 and 2014. The model was masked as a function of the data.

Figure 12: Vertical profiles of temperature ($^{\circ}\text{C}$; a), salinity (psu; b), oxygen ($\text{ml O}_2 \text{l}^{-1}$; c), nitrate (mmol N m^{-3} ; d), phosphate (mmol P m^{-3} ; e), and dissolved silica (mmol Si m^{-3} ; f) concentrations at INDOMIX cruise Station 3 (Halmahera Sea; 13 - 14 July 2010). CTD (light blue lines) and bottle (red crosses) measurements represent the conditions during cruise, 2-day model averages are shown by the black line.

Figure 13: Vertical profiles of temperature ($^{\circ}\text{C}$; a), salinity (psu; b), oxygen ($\text{ml O}_2 \text{l}^{-1}$; c), nitrate (mmol N m^{-3} ; d), phosphate (mmol P m^{-3} ; e), and dissolved silica (mmol Si m^{-3} ; f) concentrations at INDOMIX cruise Station 4 (Banda Sea; 15 - 16 July 2010). CTD (light blue

lines) and bottle (red crosses) measurements represent the conditions during cruise, 2-day model averages are shown by the black line.

Figure 14: Vertical profiles of temperature ($^{\circ}\text{C}$; a), salinity (psu; b), oxygen ($\text{ml O}_2 \text{ l}^{-1}$; c), nitrate (mmol N m^{-3} ; d), phosphate (mmol P m^{-3} ; e), and dissolved silica (mmol Si m^{-3} ; f) concentrations at INDOMIX cruise Station 5 (Ombai Strait; 16 - 17 July 2010). CTD (light blue lines) and bottle (red crosses) measurements represent the conditions during cruise, 2-day model averages are shown by the black line.

Table 1. Initial and open boundary conditions used for the INDO12BIO configuration.

Variables	Initial Conditions	OBC
NO₃, O₂, PO₄, Si	From WOA January ^a	WOA monthly ^a
DIC, ALK	GLODAP annual ^b	GLODAP annual ^b
DCHL, NCHL, PHY2, PHY1	From SeaWiFS January ^c	From SeaWiFS monthly ^c
NH₄	Analytical profile ^d	Analytical profile ^d
DOC, Fe	ORCA2 January	ORCA2 monthly

^a: From World Ocean Atlas (WOA 2009) monthly climatology, with increased nutrient concentrations along the coasts (necessary adaptation due to crucial lack of data in the studied area).

^b: Key et al. (2004).

^c: From SeaWiFS monthly climatology. Phytoplankton is deduced using constant ratios of 1.59 g Chl mol N⁻¹ and 122/16 mol C mol N⁻¹, and exponential decrease with depth.

^d: Low values offshore and increasing concentrations onshore.

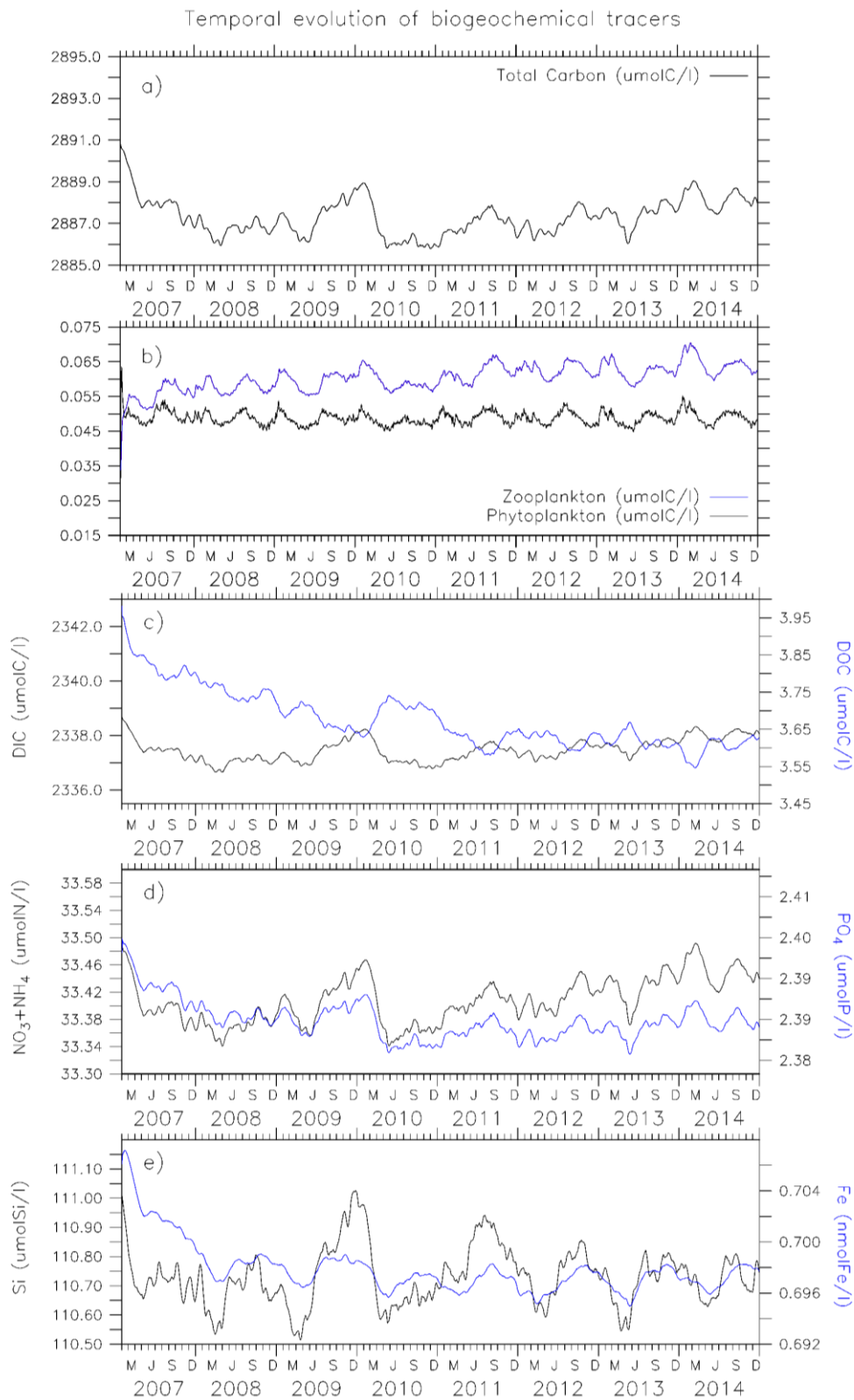


Figure 1. Temporal evolution of total carbon (a), plankton (b), DIC and DOC (c) and nutrient (d, e) content averaged over the whole 3-dimensional INDO12BIO domain.

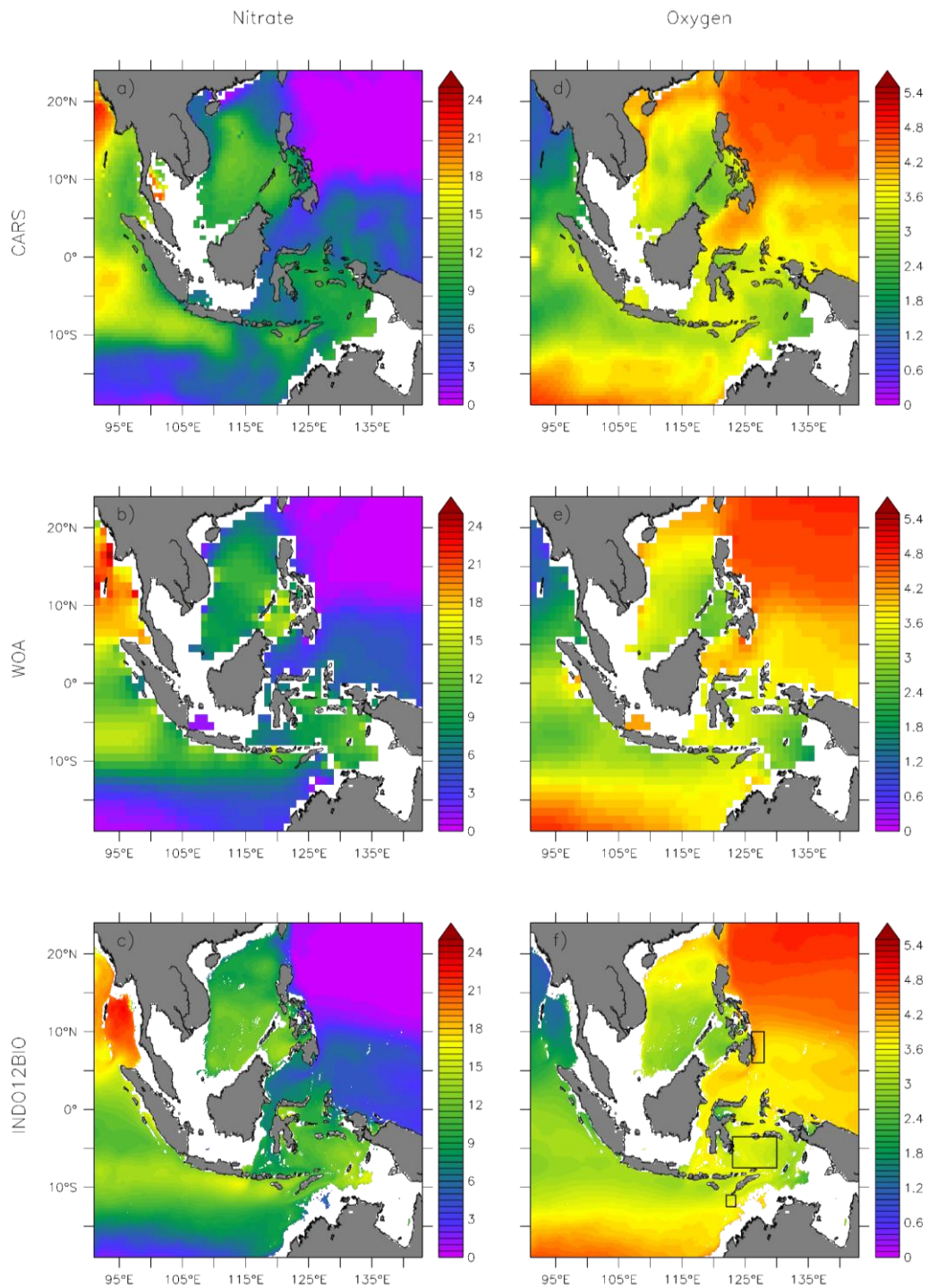


Figure 2: Annual mean of nitrate (mmol N m^{-3} ; left) and oxygen concentrations ($\text{ml O}_2 \text{l}^{-1}$; right) at 100 m depth from CARS (a, d) and WOA (b, e; statistical mean) annual climatologies, and from INDO12BIO as 2010-2014 averages (c, f). Three key boxes for water mass transformation (North Pacific, Banda, and Timor; Koch-Larrouy et al., 2007) were added to the bottom-right figure.

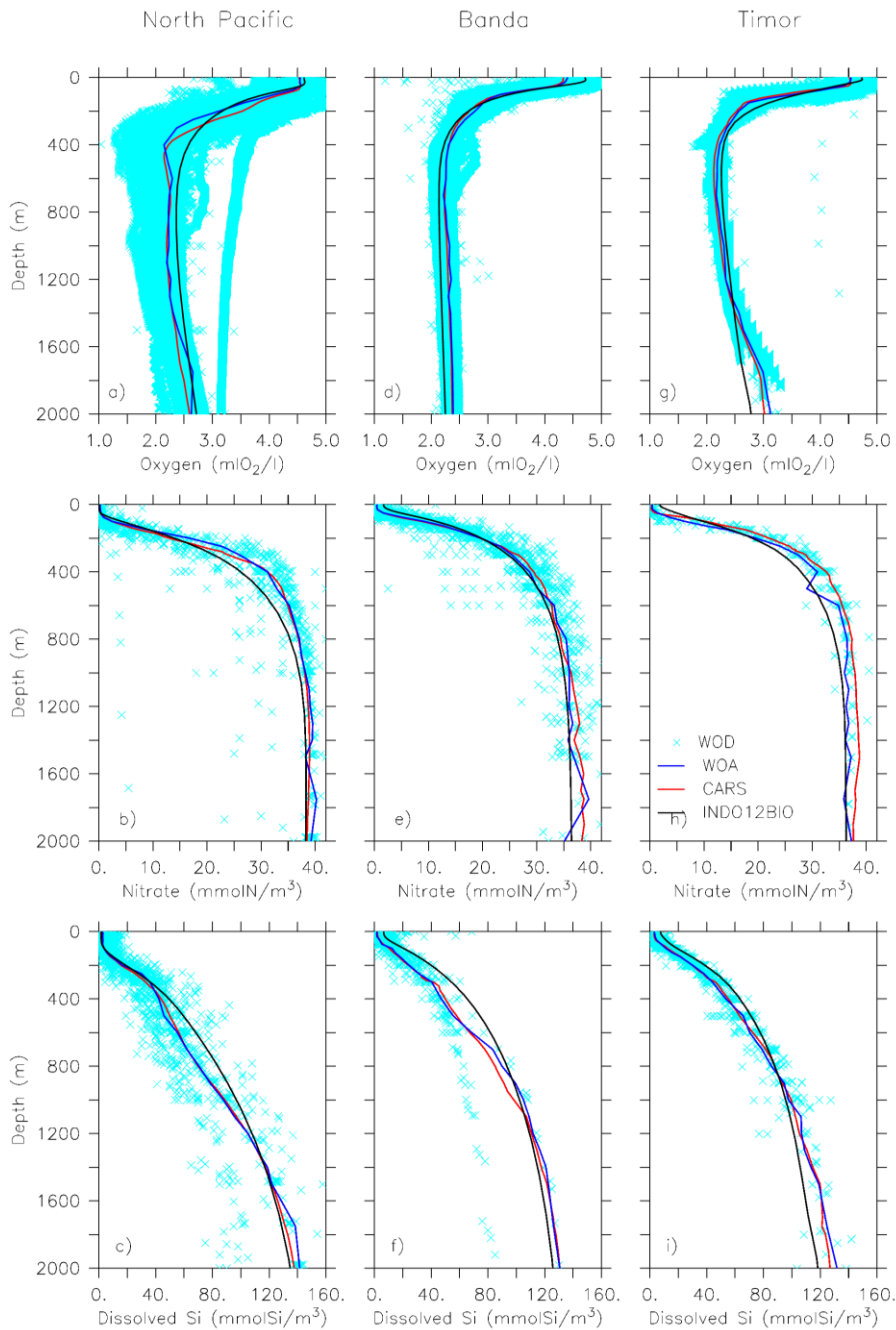


Figure 3: Vertical profiles of oxygen ($\text{ml O}_2 \text{ l}^{-1}$; top: a, d, g), nitrate (mmol N m^{-3} ; middle: b, e, h) and dissolved silica (mmol Si m^{-3} ; bottom: c, f, i) in 3 key boxes for water masses transformation (North Pacific, left; Banda, middle; and Timor, right) (see Fig. 2; Koch-Larrouy et al., 2007). CARS and WOA annual climatologies are in red and dark blue. INDO12BIO simulation averaged between 2010 and 2014 is in black. All the raw data available on each box and gathered in the WOD (light blue crosses) are added in order to illustrate the spread of data.

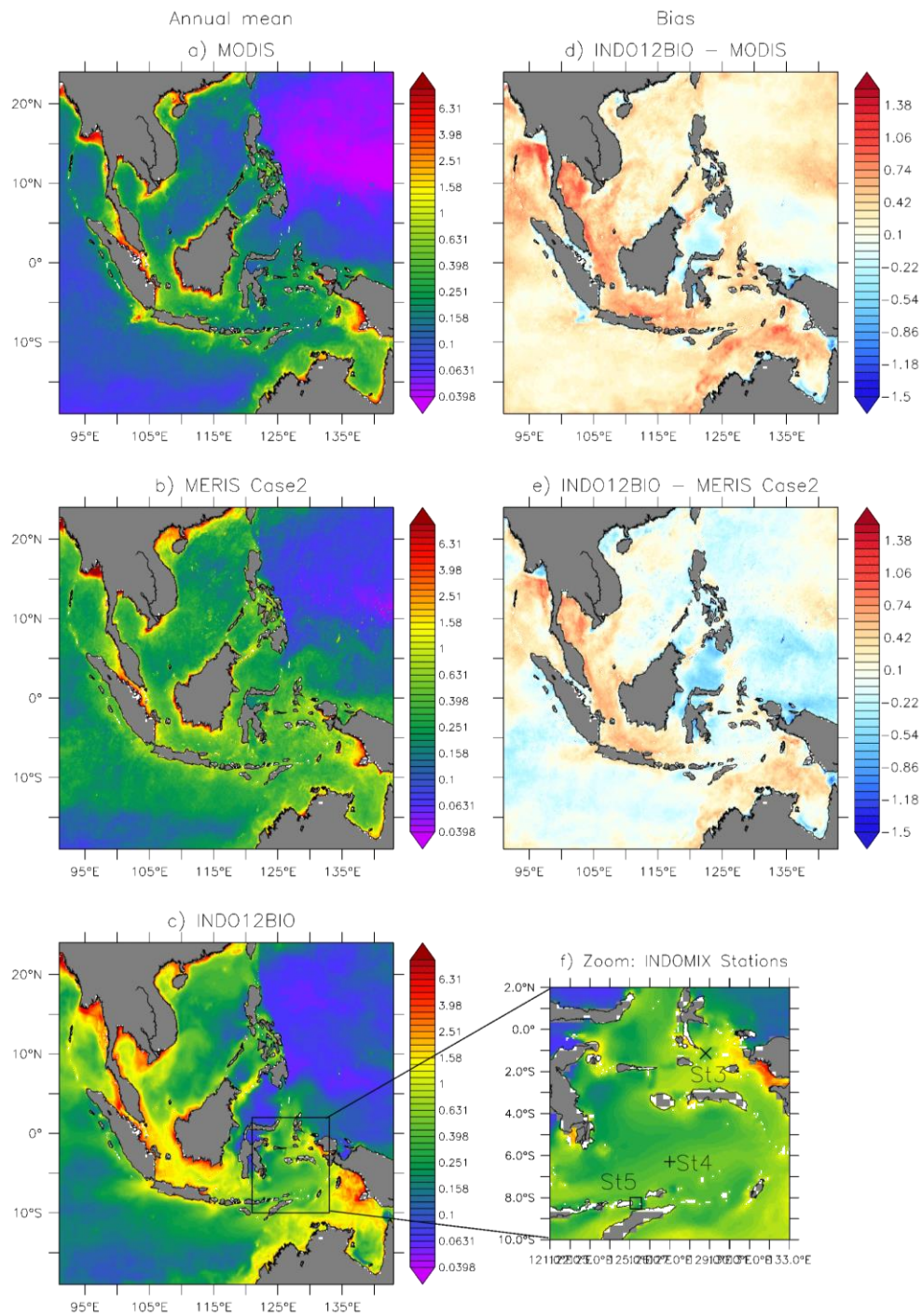


Figure 4. Left) Annual mean of surface chlorophyll-*a* concentrations (mg Chl m^{-3}) for year 2011: MODIS Case-1 product (a), MERIS Case-2 product (b) and INDO12BIO simulation (c). Right) Bias of log-transformed surface chlorophyll (model-observation) for the same year. The model was masked as a function of the observation, MODIS Case-1 (d) or MERIS Case-2 (e). Location of 3 stations sampled during the INDOMIX cruise and used for evaluation of the model in Section 4.4 (f).

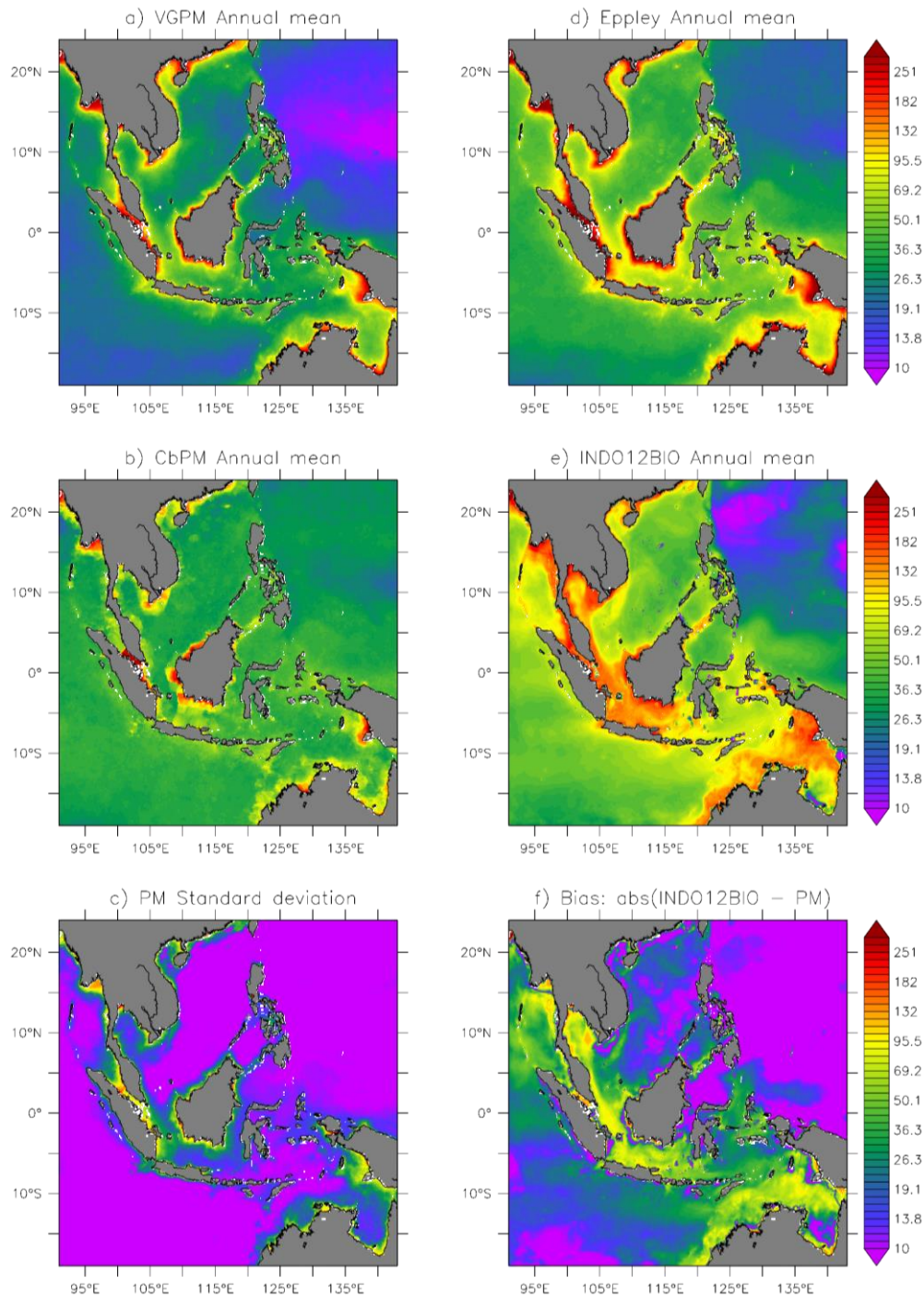


Figure 5. Annual mean of vertically integrated ~~primary production~~NPP ($\text{mmol C m}^{-2} \text{d}^{-1}$) for year 2011: VGPM (a), Eppley (d), and CbPM (b) production models, all based on MODIS ocean colour, as well as for INDO12BIO (e). Standard deviation of the 3 averaged production models (PM) (c), and bias between INDO12BIO and the averaged PM (f).

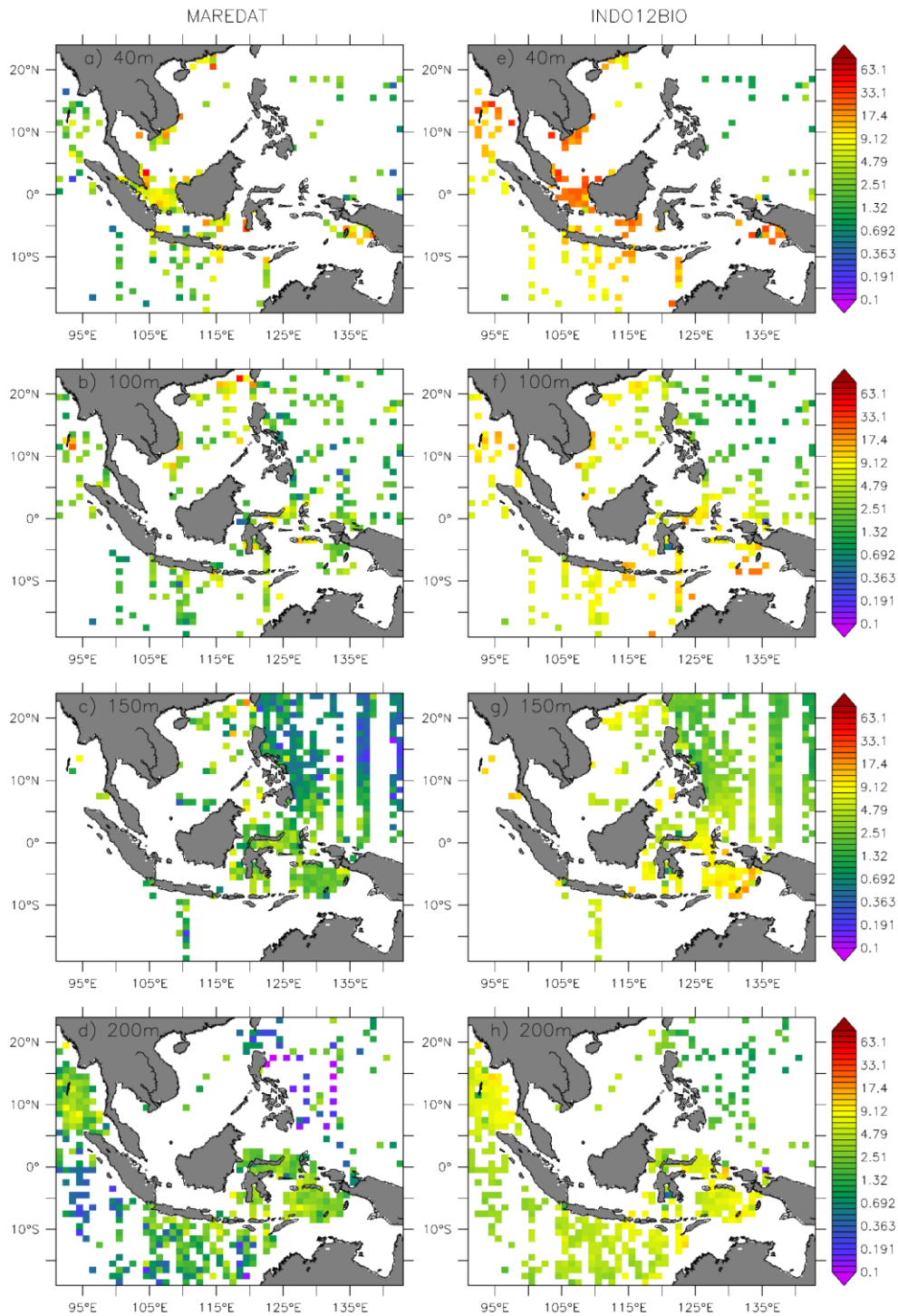


Figure 6: Annual mean of mesozooplankton biomass ($\mu\text{g C l}^{-1}$) from MAREDAT monthly climatology (left) and from INDO12BIO simulation averaged between 2010 and 2014 (right), for distinct depth interval: from the surface up to 40m (a, e), 100m (b, f), 150m (c, g), and 200m depth (d, h). Simulated fields were interpolated onto the MAREDAT grid, and masked as a function of the data (in space and time).

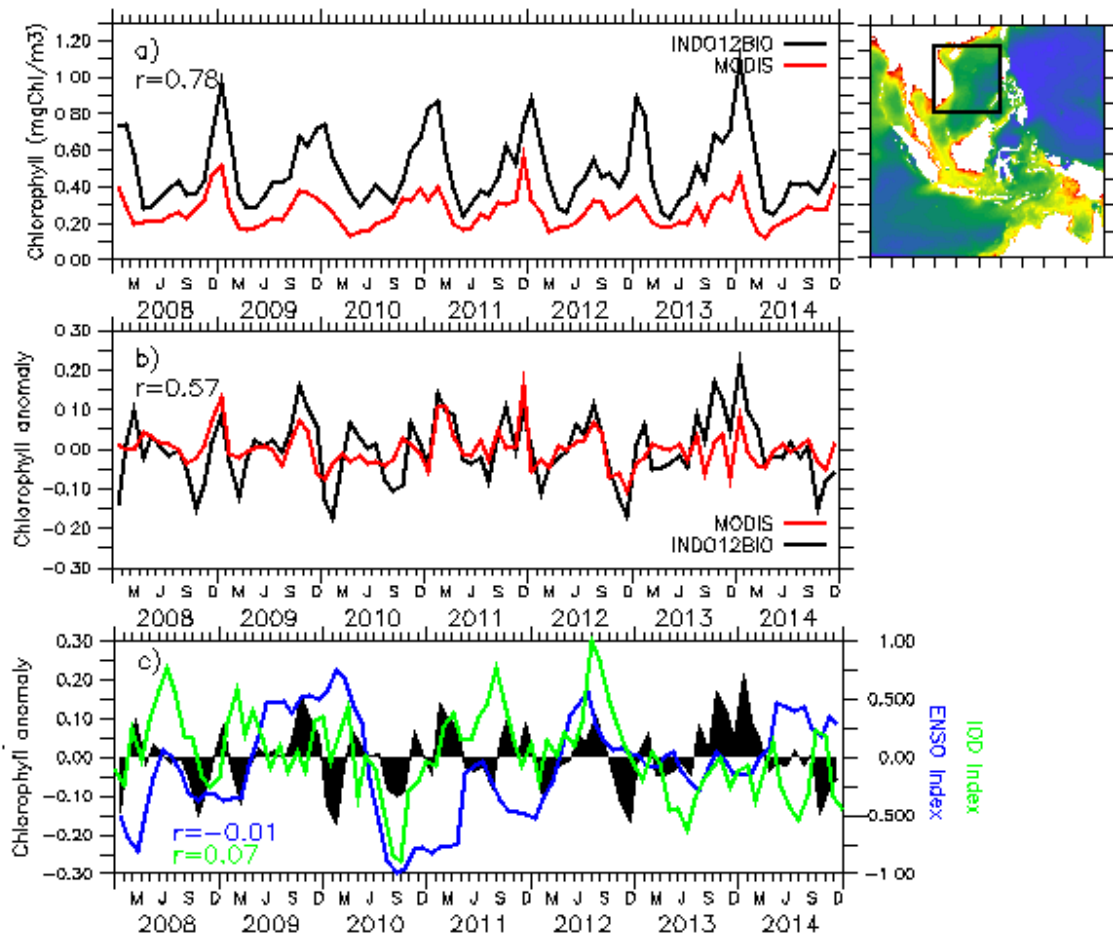


Figure 7: a) Mean surface chlorophyll-*a* concentrations and b) its interannual anomalies (mg Chl m^{-3}) over the South China Sea. INDO12BIO is in black and MODIS Case-1 in red. Temporal correlation (r) between both time series is in black. c) ENSO (blue) and IOD (green) phenomena are respectively represented by MEI and DMI indexes. Indexes were normalized by their maximum value in order to be plotted on the same axis. Interannual anomalies of simulated chlorophyll-*a* reminded in black. Temporal correlation (r) between the simulated chlorophyll-*a* and ENSO (IOD) is indicated in blue (green).

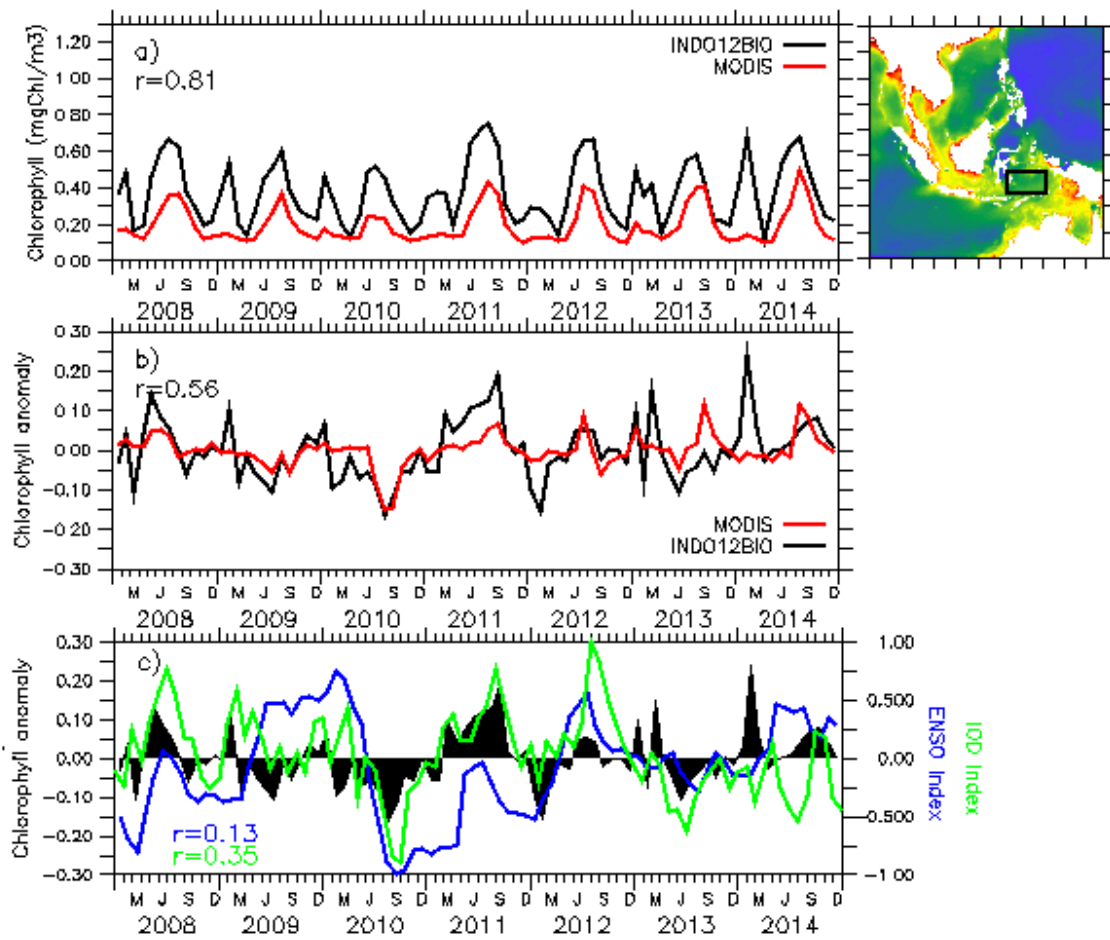


Figure 8: Same as Figure 7, in Banda Sea.

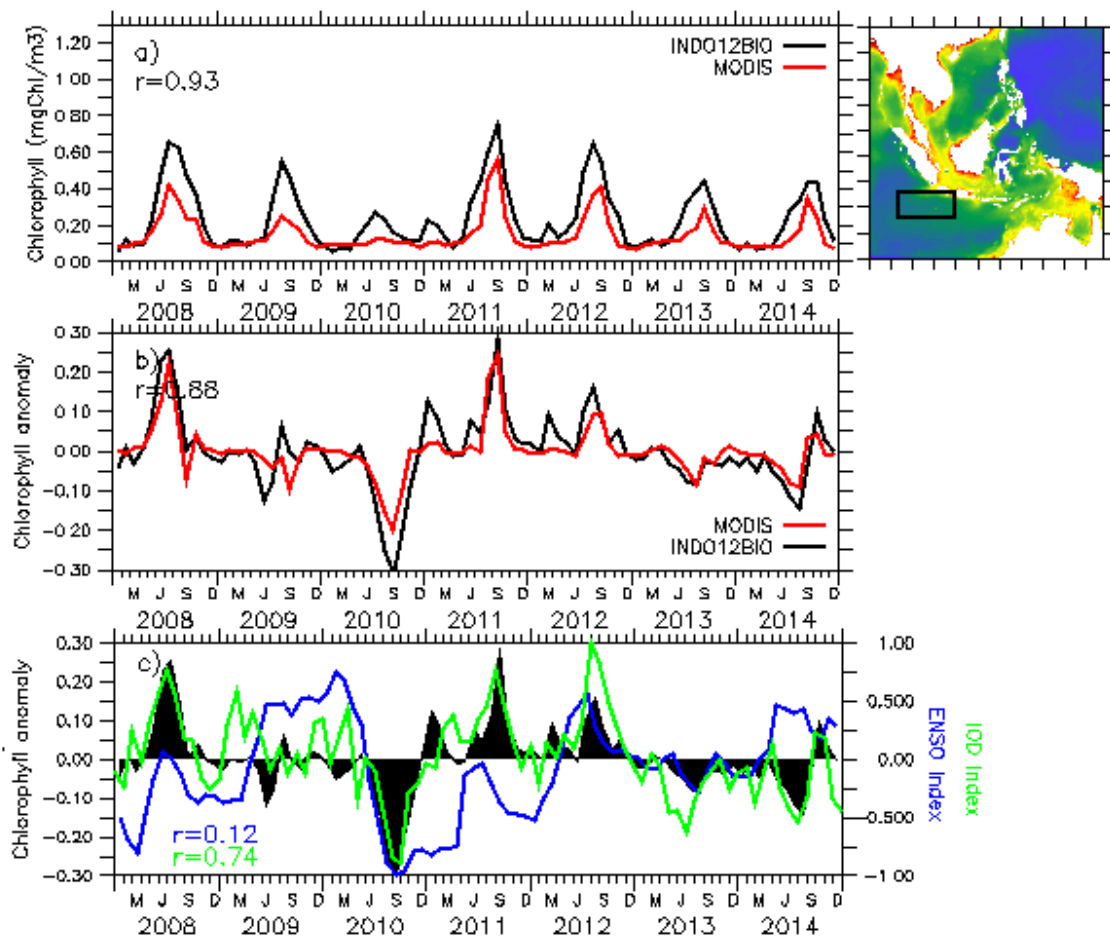


Figure 9: Same as Figure 7, in Sunda area.

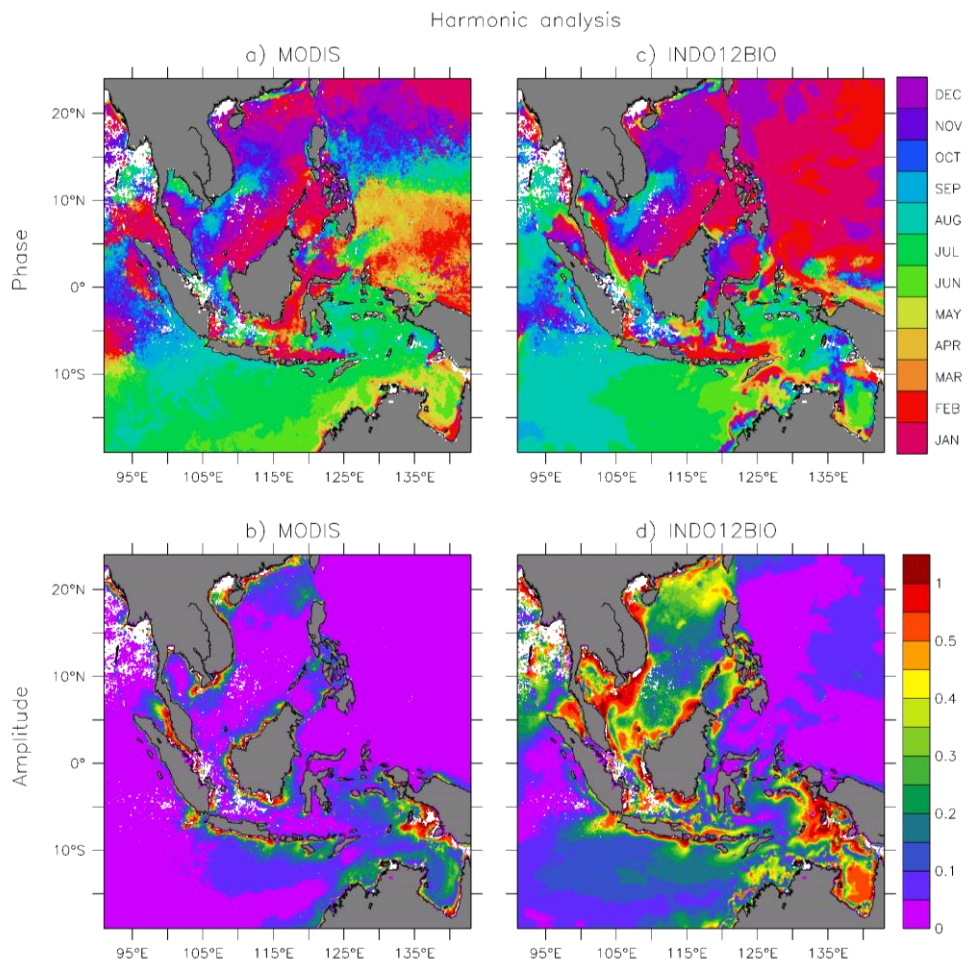


Figure 10. Timing of maximum chlorophyll-*a* (a, c) and amplitude (b, d) for a monthly climatology of surface chlorophyll-*a* concentrations between 2010 and 2014: MODIS Case-1 (left) and INDO12BIO (right). The model was masked as a function of the data.

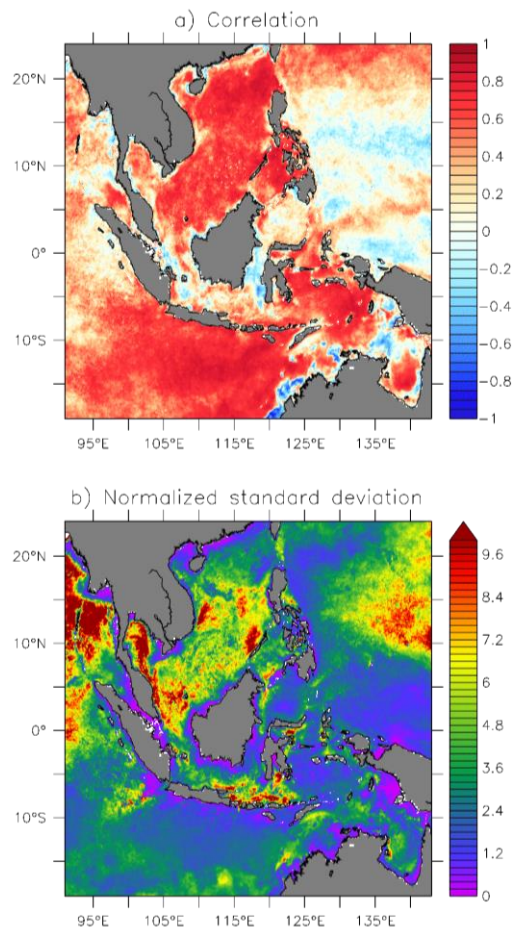


Figure 11: Temporal correlation (a) and normalised standard deviation (b; $\text{std}(\text{model})/\text{std}(\text{data})$) estimated between the INDO12BIO simulation and the MODIS Case-1 ocean colour product. Statistics are computed on monthly fields between 2010 and 2014. The model was masked as a function of the data.

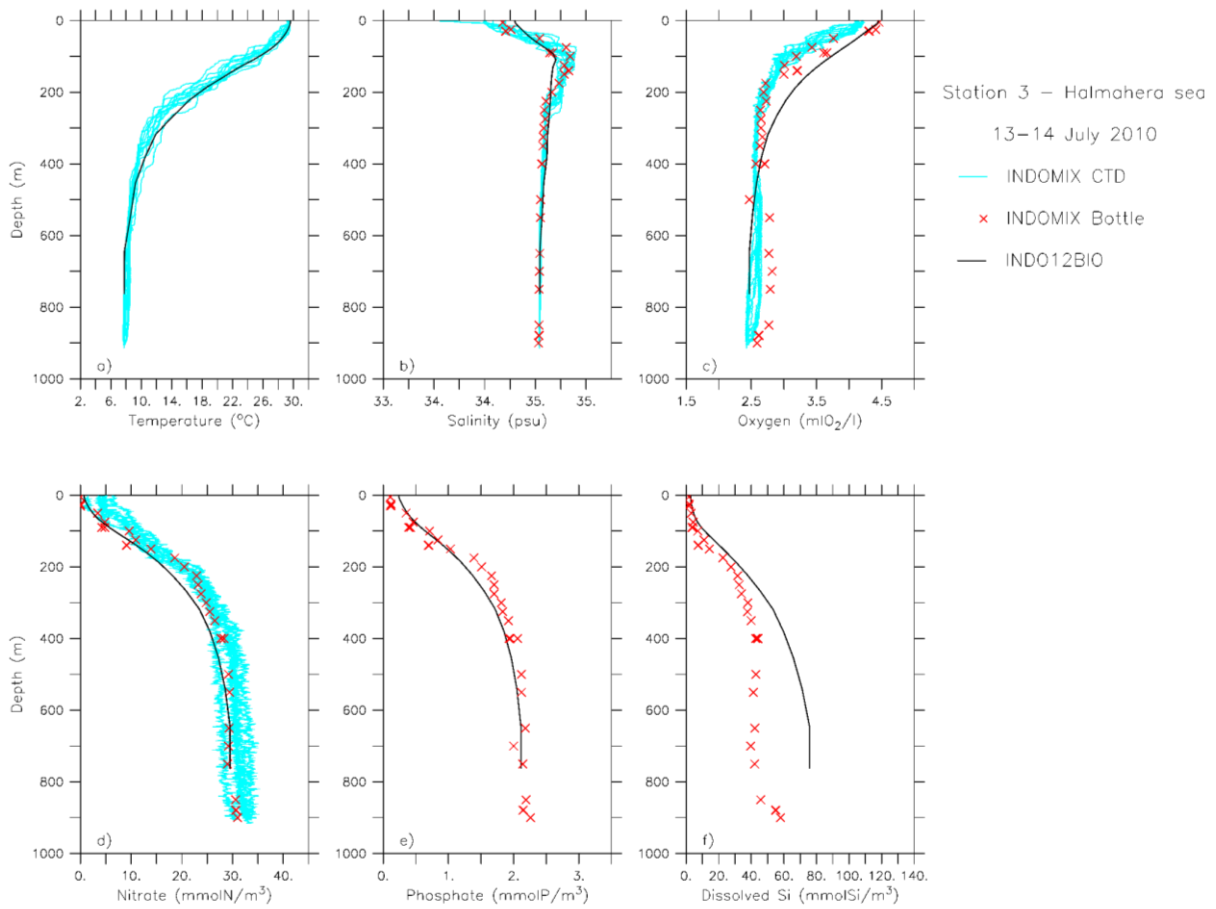


Figure 12: Vertical profiles of temperature ($^{\circ}\text{C}$; a), salinity (psu; b), oxygen ($\text{ml O}_2 \text{ l}^{-1}$; c), nitrate (mmol N m^{-3} ; d), phosphate (mmol P m^{-3} ; e), and dissolved silica (mmol Si m^{-3} ; f) concentrations at INDOMIX cruise Station 3 (Halmahera Sea; 13 - 14 July 2010). CTDO or ISUS sensor (light blue lines) and bottle (red crosses) measurements represent the conditions during cruise, 2-day model averages are shown by the black line.

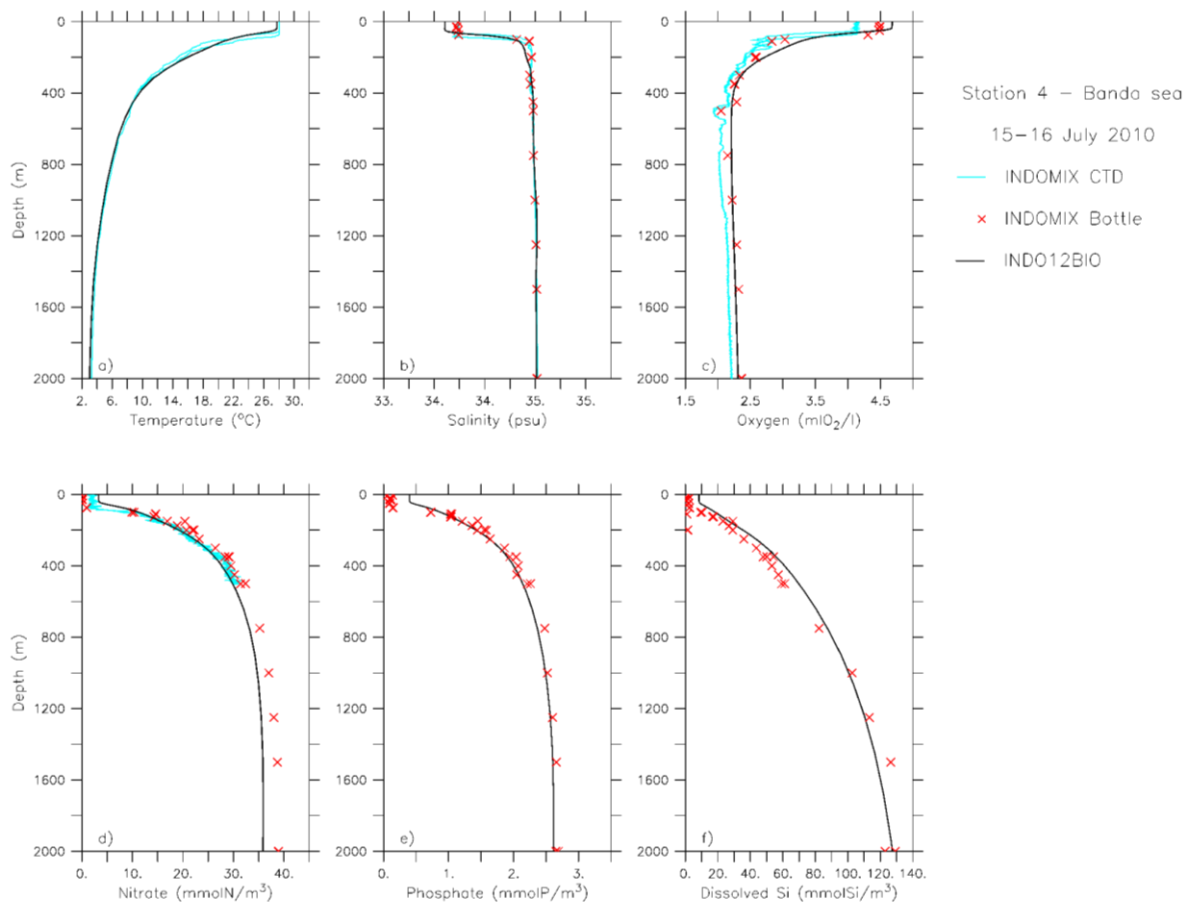


Figure 13: Vertical profiles of temperature ($^{\circ}\text{C}$; a), salinity (psu; b), oxygen ($\text{ml O}_2 \text{ l}^{-1}$; c), nitrate (mmol N m^{-3} ; d), phosphate (mmol P m^{-3} ; e), and dissolved silica (mmol Si m^{-3} ; f) concentrations at INDOMIX cruise Station 4 (Banda Sea; 15 - 16 July 2010). CTDO or ISUS sensor (light blue lines) and bottle (red crosses) measurements represent the conditions during cruise, 2-day model averages are shown by the black line.

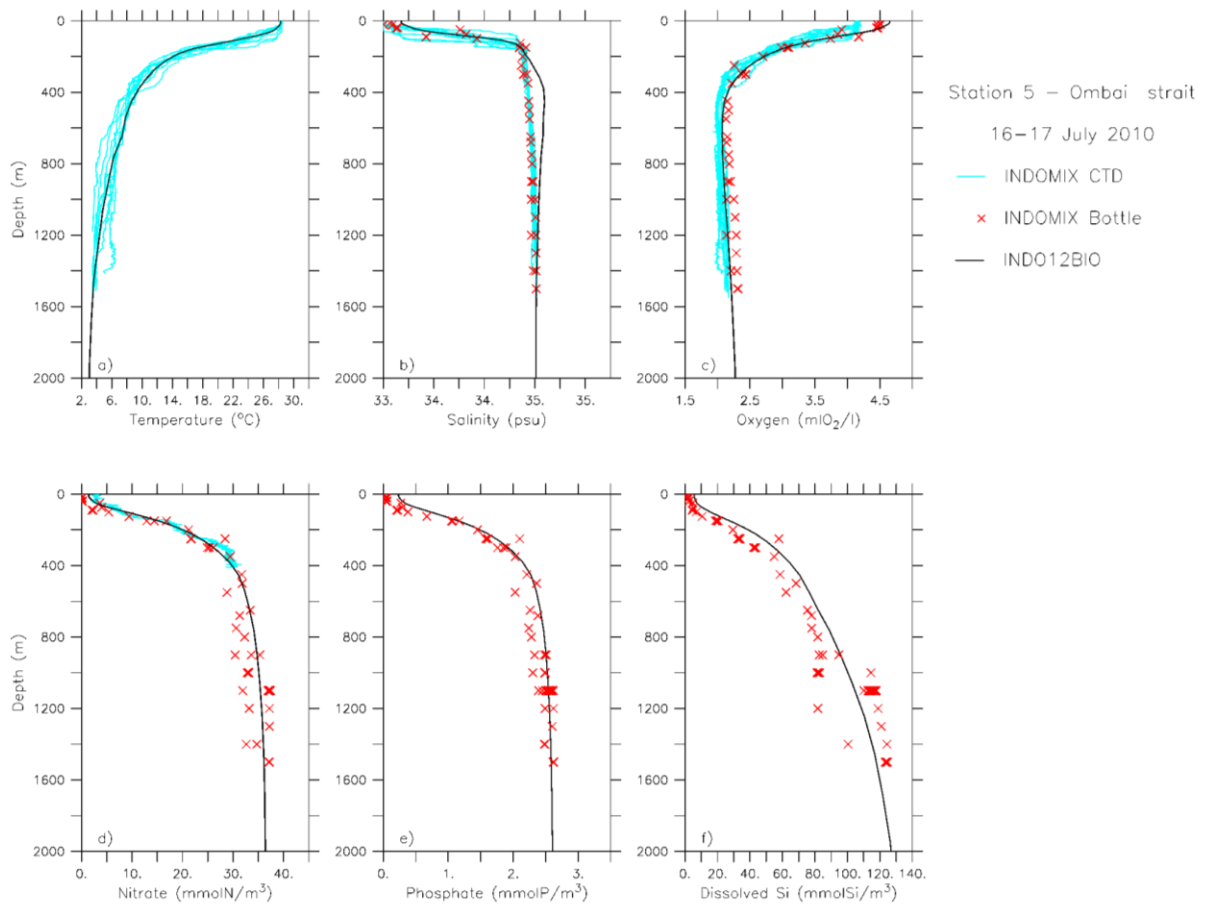


Figure 14: Vertical profiles of temperature ($^{\circ}\text{C}$; a), salinity (psu; b), oxygen ($\text{ml O}_2 \text{ l}^{-1}$; c), nitrate (mmol N m^{-3} ; d), phosphate (mmol P m^{-3} ; e), and dissolved silica (mmol Si m^{-3} ; f) concentrations at INDOMIX cruise Station 5 (Ombai Strait; 16 - 17 July 2010). CTDO or ISUS sensor (light blue lines) and bottle (red crosses) measurements represent the conditions during cruise, 2-day model averages are shown by the black line.